PROTEINS CONTROL IN BIOMINERALIZATION PROCESSES OF THE FRESHWATER PEARL MUSSEL *HYRIOPSIS CUMINGII*

Dissertation
zur Erlangung des Grades
Doktor der Naturwissenschaften
im Promotionsfach Pharmazie

Am Fachbereich Chemie, Pharmazie und Geowissenschaften
der Johannes Gutenberg-Universität
in Mainz

Antonino Natoli
geb. in Palermo (Italien)

Mainz, 12.05.2009

Tag der mündlichen Prüfung: 12.05.2009

1. INTRODUCTION

1.1. Biomineralization

Since the Cambrian (approx. 540 million years ago) organisms started to form minerals in a controlled way; this ability named "***biomineralization***" evolved during the time providing to eukaryotes and prokaryotes perfect tools for defense, feeding, storage, mechanical support and orientation (Weiner S., 2003). Due to their complexity, the study of these biogenic materials needs a multidisciplinary approach that involves biology, physics, chemistry, crystallography, biochemistry and medicine. The main characteristic of a biomineral is the association of the inorganic phase with an organic matrix that plays a central role for determining unique final features. The organic portion has some common components found in almost all biominerals, as proteins, collagen, chitin, polysaccharides and mucopolysaccharides. Negatively charged and glycosilated proteins are the most interesting and investigated biochemical tools for mineralization especially the ones involved in calcium carbonate precipitation. Compared to the mineral part, the organic matrix is represented in a very small percentage, in calcium carbonate biominerals for example it is less than 5% (Marin F., 2004), but nevertheless its effect is extraordinary. Biogenic minerals in fact, have not only amazing shapes and beautiful colors but also enhanced chemical and physical properties compared to pure inorganic minerals (Wheeler A.P., 1984; Matsushiro A., 2004; Blank S., 2003; Falini G., 1996).

The biologically induced mineralization can regulate shape, size and orientation during crystals growth, helping also the stabilization of metastable polymorphs, as the amorphous phases of silica or high energetic forms of calcium carbonate like vaterite and aragonite, generally all unstable in water solution. The organic matrix allows also an enzyme-mediate synthesis under normal environmental conditions of pressure and temperature, as in spiculae of siliceous sponges, where a protein called *silicatein* can produce amorphous silica; without proteins control this polymerization is possible only

under extreme values of pH, temperature and pressure (Müller W.E.G., 2005). The so formed biocomposites have a defined and ordered structure; a typical arrangement is the one present in mollusk shell and called "*brick and mortar*" in which regular crystals of aragonite represent the bricks while the mortar is constituted by the surrounding organic matrix (Addadi L., 1997); this complex, self-assembling architecture results in amazing mechanical performances as high flexibility and fracture resistance, even 3000 times greater in comparison with the corresponding synthetic and geological minerals (Levi C., 1989; Currey J.D., 1980).

For these reasons, the biocomposites more than inorganically formed materials, find promising applications in several fields as clinic, nanotechnologies, material science and biomimetic engineering (Fendler J.H., 1997; Kaplan D.L., 1998; Hou W.T., 2006; Sarikaya T., 1999).

1.2. Types of Biominerals

A large variety of biominerals can be distinguished in many organisms from the most simple as bacteria to most evolved as humans. More than 60 types of biomaterials were classified according to their inorganic components (Lowenstam H.A., 1989).

1.3. Calcium Biominerals

Calcium is a fundamental element involved in many metabolic cellular processes, it is also represented in about 50% of known biocomposites; calcium phosphate and calcium carbonate are the most important and abundant biominerals on the Earth. The former as hydroxyapatite ($\mathbf{Ca_{10}(PO_4)_6\,(OH)_2}$) is the constituent of vertebrate skeleton and teeth, while the latter forms spicules, eggshells and the exoskeleton of many invertebrates.

Calcium carbonate (**$CaCO_3$**) produced as biomaterial in aquatic animals, due to the large amount and distribution, acts as an important reservoir of calcium and as pivotal regulator in the carbonate biogeochemical cycle, participating also to climate regulation and Earth's homeostasis. It also provides a potential chemical energy source due to the endothermic decomposition reaction in CaO and CO_2 (Wilt F.H., 2007; Barker R., 1973; Barker R., 1974). Recently calcium carbonate biominerals attracted the attention of geochemists, palaeontologists and archaeologist as records for reconstruction of climatic changes and study of global warming (Weiner S., 2008).

Calcium carbonate can occurs in different forms: ***amorphous calcium carbonate*** (ACC) is the most unstable and soluble form (Weiner S., 2003), it can be formed in early development stages as precursor of the crystalline phases like in immature endoskeletal spicules of sea urchin larvae (Weiss I.M., 2002; Wilt F.H., 1999), in larval shells of marine bivalves, in cuticles of isopods and terrestrial and marine crustacean (Becker A., 2005). ACC can also be found in stabilized forms having mechanical and storage functions, for example in plant leaves as intracellular calcified bodies (cystoliths) or in ascidians skeleton (Taylor M.G., 1993; Ainzeberg J., 2002).

In aqueous solution within minutes amorphous calcium carbonate reprecipitates in three crystalline polymorphs. The first is the high energetic ***vaterite*** that in some hours undergoes to transformation to the most thermodynamically stable ***calcite***, passing through ***aragonite*** (Bischoff J. L., 1968; Nehrke G., 2006). Aragonite and calcite are the most diffused polymorphs produced by living organisms; the former is present in the exoskeleton of Cnidarians and in tropical algae as deposit, while the latter forms spinal and skeletal elements of Echinoid, spicules of Calcarea, exoskeleton of crabs and lobsters and coccoliths plates in coccolithophores. In mollusks, like the pearl oyster *Pinctada fucata* or the red abalone *Haliotis rufescens*, both polymorphs are synthesized: aragonite constitutes the inner nacreous layer while the outer part of the shell is made of calcite (Bosselmann F., 2007; Jeremy R., 2003; Meyer K.D., 1995; Fu G., 2005; Matsushiro A., 2004, Young J.R., 2003).

Vaterite, due to its high thermodynamic instability, is very rare in nature and acts mostly as precursor of aragonite and calcite; in some organisms it can be found in small amount in association with the other calcium carbonate polymorphs: as in human gallstones, ascidians spicules, fish otoliths and in repaired portions of the mollusk shells

(Lowenstam H.A., 1997; Palchik N.A., 2005; Falini G., 2005; Oliveira A.M., 1996; Mayer, 1932). Recently vaterite was described in freshwater pearls from Chinese and Japanese mollusks, as relatively common component that can influence their final quality (Qiao L., 2007; Wehrmeister U., 2007; Ma H.J., 2006).
Other biominerals containing calcium can be found in higher plants, in the form of oxalate (**CaC_2O_4**) crystals used as defense against herbivore and reservoir for calcium (Webb M.A, 1999), or as sulfate (**$CaSO_4$**) in medusa as component of the complex receptorial organ called *rhopalium* (Becker A., 2005).

1.4. Other Biominerals

Silicon is the second most abundant element in the Earth's crust. Amorphous silica (**SiO_2**) is the main constituent of sponge spicules of Demospongiae and Hexactinellida (Müller W.E.G., 2007d) and of the cell walls (*frustule*) of the diatoms; the amazing shapes of these unicellular eukaryotic algae are an example of how surprising biomaterials are (Kroeger N., 2007d; Robinson D.H., 1987; Swift D.N., 1992).

Iron complex as magnetite (**Fe_3O_4**) or greigite (**Fe_3S_4**) are synthesized from magnetotactic bacteria; nanocrystals of these iron sulfides and oxides are stored in membrane vesicles and used for orientation and migration along magnetic field lines (Bäuerlein E., 2003; DeLong E.F., 1993; Frankel R.B., 1979).

1.5. Pearls

Pearls represent a precious and sophisticated example of biomineralization process that fascinated human being since antiquity. One of the oldest jewels containing them, called *"the Susa necklace"*, was found in the sarcophagus of a Persian princess who died in 520 BC (Museum du Louvre, Paris). Pearls have already been studied in the ancient

Greek period by the philosopher Theophrastus (372-278 BC) that in his book *Περὶ Λίθων* defined them "precious stones". For Sumerians and pre-Columbian Americans these biological gems became important symbols of wealth, status and religious belief. In 500 A.D. the Chinese were used to place inside of the mussels small Buddha's figures in order to produce blister pearls, this was the first attempt of artificial production. In the middle of the 18th century Linnaeus carried several successful experiments that culminated with the first 'artificial' spherical pearl. He drilled a small hole in the shell of the freshwater mussel *Unio pictorum* and in order to keep the irritant nuclei away from the shell inner surface, he inserted a T-shaped piece of silver wire *(Linnaeus and the production of artificial pearls*. Nature, 1930). In this way the nacre was deposited around the seed obtaining a free pearl rather than a blister one. But the fame of artificial pearls is linked to the Japanese Kokichi Mikimoto (1858-1954). During his life he played the major role in both developing modern techniques for culturing pearls and convincing the general public to accept those pearls precious and valuable as the natural ones. His efforts opened new markets worldwide and essentially created the pearl industry that exists today. Natural pearls are very rare and they are formed as a defence response when an irritant enters in contact with the pearl mussel. Small organic and inorganic particles as sand, parasites, part of animals or algae, can enter in the shell during feeding or respiration processes; the resulting contact acts as stimulus for a unique biomineralization process. The epithelial cells of the mantle, as response, encapsulate the foreign body forming the "pearl-sac" and start to secrete the nacre (mother of pearl) which layer by layer will generate the pearl. In order to produce cultured pearls for commercial purposes, this natural process during the centuries has been artificially developed and optimized, together with mussels farming (Wada K., 1998; Akamatsu S., 2001). High specialized operators are able to open the shell with care and place the nucleus in a pocket obtained by cutting the mantle or the gonad of the mollusc (fig. 1).

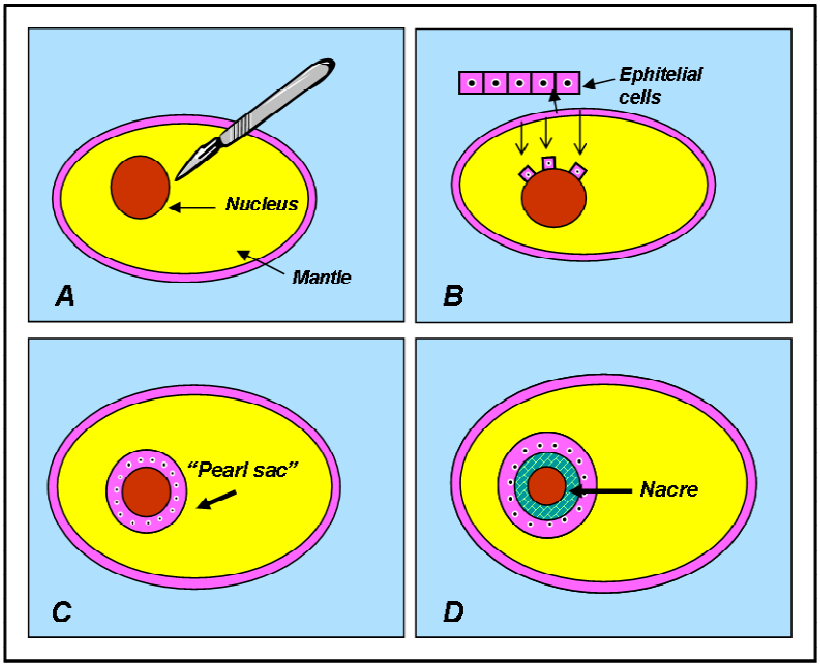

Fig. 1: Representation of cultured pearl production: after opening the animal valves, the nucleus is grafted in the mantle lobe (A), as response the epithelial cells start to migrate around the foreign body (B). Once the "pearls sac" is formed (C), the surrounding cells produce nacre that encapsulates the nucleus and generates the pearl.

Although the traditional sources of pearls have been oysters living in saltwater, gradually fresh- and sea-water pearls reached a comparable production, quality and popularity. The primary difference between freshwater cultured pearls (FWCPs) and the seawater ones (SWCPs) is the type and the number of irritating nuclei introduced for promoting pearl production. In freshwater mussels up to 50 small pieces of mantle tissue from another specimen can be implanted by cutting the living mantle, this pieces are thin about 2 mm and they are rolled as round as possible before insertion. In seawater oysters only one nucleus bigger than the one of the freshwater and consisting of a bead obtained from another shell, is grafted in the reproductive organ. This difference determines the final characteristics of the pearls. Seawater cultured usually have a perfect shape due to the geometry of the bead nucleus, freshwater ones are unique for the huge variety of shapes and colors, having also thicker and more resistant nacre due to the absence of nuclei that determines an "all-pearl". The culturing periods

are as well different: a FWCP needs from 2 to 5 years to be completely formed while a SWCP is ready in less than a year. Nowadays the main producers of cultivated pearls are Japan, China, Australia, U.S.A. and Tahiti. The 95% of the world market of freshwater pearls is controlled by China with a production of 1800 tons per year (Dan H., 2002). The affordable prices are rendering Chinese pearls accessible to the mass market in both developed and developing countries, in 2004 the Chinese production value was 150 million (US$), about 24% of the world's total fresh and sea water pearls market (source: SPC Pearl Oyster Information Bulletin, number 7 – November 2006). In all parts of China approximately 167,000 km^2 (Strack E., 2001) among natural and artificial ponds, rivers and lakes are exploited for FWCPs cultivation. The most diffused and used animal in Chinese freshwater farming is the "triangle mussel" *Hyriopsis cumingii*, pretty much common in the largest lakes: Poyanghu Lake, Dongtinghu Lake, Taihu Lake, Chaohu Lake and Hongzehu Lake. Since the end of the 20^{th} century this mussel has gradually replaced the "comb mussel" *Cristaria plicata* (Li J., 2007), yielding high quality pearls with better luster, smoother surface, rounder shape and bigger size. In a standard *Hyriopsis cumingii* mussel (10 cm in length) about 25-30 slices (3 mm x 3 mm) of mantel tissue from another specimen can be implanted by cutting the fleshy mantel lobe. Produced pearls have a wide color range and size from 2 mm to 13 mm. After harvesting, the same mussels can be seeded again and placed back in the water for a new production.

2. AIM OF THE STUDY

Living organisms are able to synthesize mineralized structures, composed by an inorganic phase and an organic one. This hybrid framework gives them amazing and unique features. In the present PhD work we wanted to deep our knowledge on calcium carbonate biomineralization processes. The pearls of the Chinese freshwater mollusc *Hyriopsis cumingii* were chosen as starting material, due to the wide diffusion and the relevance of their worldwide market value. In particular we wanted to emphasize the role of the proteins contained in the organic portion of the biomineral. A wide outstanding literature postulated the ability of acidic and glycosilated proteins to control the crystallization of calcium carbonate in molluscs calcitic shell. In the past years a great interest was showed especially on the proteins extracted from the nacreous layers of marine molluscs, in which aragonite revealed enhanced physical-chemical properties compared to the synthetic or geological one. But so far, no data has been reported on the organic matrix composition of freshwater pearls. The organic matrix is considered as the main responsible of the extraordinary features of biomaterials by means of its regulatory effect during crystals formation. Another extremely interesting aspect of biomineralization is the ability of selection between different polymorphic forms of calcium carbonate. The occurrence of all three crystalline polymorphs of $CaCO_3$ in pearls and shells of *Hyriopsis cumingii* has thus stimulated our curiosity. In the specific the presence of the high energetic vaterite in this kind of pearls, is quite unique for the amount and for its physical characteristics. The study of the structural and functional aspects of the polypeptides involved in crystals formation and polymorphs stabilization is the main key to understand biomineralization processes and optimize innovative tools for production of new bio-inspired materials.

3. MATERIALS AND METHODS

3.1. Chemicals

2-Mercaptoethanol	Sigma, Steinheim
5-Brom-4-chlor-3-indolyphosphat disodium salt (BCIP)	Carl Roth, Karlsruhe
Acetic acid	Carl Roth, Karlsruhe
Albumin from bovine serum, fraction V	Carl Roth, Karlsruhe
Ammonium carbonate	Sigma, Steinheim
Ammonium peroxydisulphate (APS)	Sigma, Steinheim
Anti-rabbit IgG (Fab specific)-alkaline phosphatase antibody produced in goat	Sigma, Steinheim
Anti-rabbit IgG Cy3-conjugated Ab	Dianova, Hamburg
Anti-rabbit IgG Gold antibody produced in goat	Sigma, Steinheim
Araldit Rapid	Carl Roth, Karlsruhe
Avidin-alkaline phosphatase	Sigma, Steinheim
BCIP (5-bromo-4-chloro-3-indolyl phosphate disodium salt)	Sigma, Steinheim
Biolyte-ampholytes	Biorad, Hercules
Borate buffer	PIERCE, Rockford
Bromophenolblue	Sigma, Steinheim
Calcium chloride	Carl Roth, Karlsruhe
Carbonic anhydrase from bovine erythrocytes	Sigma, Steinheim
Deoxycholic acid	Sigma, Steinheim
Dimethylformamide (DMF)	PIERCE, Rockford
Dithiothreitol (DTT)	Biorad, Hercules
Dowex 50WX8	Fluka, Buchs

Enzymatic Carborelease Kit	QA-Bio, San Mateo
Ethanol	Sigma, Steinheim
Ethylenediaminetetraacetic acid (EDTA)	Carl Roth, Karlsruhe
EZ-Label FITC Protein Labeling Kit	PIERCE, Rockford
Fetuin	QA-Bio, San Mateo
Formaldehyde	Carl Roth, Karlsruhe
Formamide	Carl Roth, Karlsruhe
Freund's Adjuvant complete	Sigma, Steinheim
Freund's Adjuvant incomplete	Sigma, Steinheim
Fuchsin-sulfite (Schiff's) reagent	Sigma, Steinheim
Gelcode Blue Stain Reagent	Pierce, Rockford
Glycerol	Carl Roth, Karlsruhe
Glycine	Carl Roth, Karlsruhe
Glutharaldehyde	Carl Roth, Karlsruhe
Hydrochloridric acid	Carl Roth, Karlsruhe
Iodoacetamide	Biorad, Hercules
Isopropanol	Carl Roth, Karlsruhe
Lectin from *Triticum vulgaris* biotin conjugated	Sigma, Steinheim
Low melting point Agarose	Sigma, Steinheim
Methanol	Carl Roth, Karlsruhe
Mineral oil	Biorad, Hercules
N,N,N',N'-Tetramethylethylenediamine, 1,2-bis(dimethylamino)-ethane (TEMED)	Carl Roth, Karlsruhe
N,N-dimethylformamide	Sigma, Steinheim
Nitrotetrazolium blue chloride (NBT)	Carl Roth, Karlsruhe
NP-40	Sigma, Steinheim
PBS buffer	Applichem, Darmstadt
Periodic acid	Carl Roth, Karlsruhe
Phosphate-buffered-saline (PBS)	Applichem, Darmstadt
p-nitrophenylacetate	Sigma, Steinheim

Polyvinylpirrolidone	Sigma, Steinheim
Potassium metabisulfite	Sigma, Steinheim
Proteinase Inhibitor Cocktail, Complete	Roche, Penzberg
ReadyPrep 2-D Cleanup Kit	Biorad, Hercules
Rothiphorese Gel 40	Carl Roth, Karlsruhe
Roti-Quant	Carl Roth, Karlsruhe
Silver Enhancer Kit	Sigma, Steinheim
Silver Stain Kit	Biorad, Hercules
Sodium bicarbonate	Sigma, Steinheim
Sodium chloride	Carl Roth, Karlsruhe
Sodium hypochlorite	Carl Roth, Karlsruhe
Sodiumdodecylsulphate	Carl Roth, Karlsruhe
Stains-All	Sigma, Steinheim
Tris-(hydroxymethyl)-amino methane	Applichem, Darmstadt
Triton X-100	Carl Roth, Karlsruhe
Tween-20	Carl Roth, Karlsruhe
Urea	Carl Roth, Karlsruhe
Western Blocking Reagent	Roche, Mannheim

3.2. Markers

PeqGold Protein Marker I	PeqLab, Erlangen
Precision Plus, Dual Color	Biorad, Hercules
2-D PAGE Marker	Biorad, Hercules

3.3. Equipments

0,2 µm sterile filters	Whatman, Dassel
Amicon Ultra-15, centrifugal filter units	Millipore, Bedford

Assay plate 96 well	Falcon, Franklin Lakes
Desiccator 0,7 L	Carl Roth, Karlsruhe
Eppendorf centrifuge 5402	Eppendorf, Hamburg
Heat block Thermostat 5320	Eppendorf, Hamburg
Heraeus Biofuge fresco	Kendro, Hanau
Hotplate/Stirrer	IKA Labortechnik, Staufen
Immobilon-P PVDF membrane	Millipore, Bedford
Lab-Tek chamber slide systems	Nalge Nunc Int., Naperville
Light microscope AHBT3 with AH3-RFC reflected light fluorescence	Olympus, Hamburg
Mini Protean II	Biorad, Hercules
Microscope glass slides	Carl Roth, Karlsruhe
Mini-Protean 3 Dodeca Cell	Biorad, Hercules
Multitemp II 2219 thermostatic circulator	LKB, Bromma
Odyssey Infrared Imaging System	LI-COR Biosciences, Bad Homburg
pH-meter CG 840	Schott, Mainz
Pipettes (2, 10, 20, 100, 200, 1000 µl)	Gilson, Middleton
Pyrex test tubes with screw cap (500ml)	Schott, Mainz
Power Pac Universal	Bio-Rad, Hercules
Protein IEF Cell	Biorad, Hercules
ReadyStrip Strip pH 4/7	Biorad, Hercules
Servapor dialysis tubing (3.5 kDa MWCO)	Serva, Heidelberg
Shaker Certomat-R	Braum Biotech, Dahn
Spectrophotometer Titertek Multiskan Plus	Bartolomey Labortechnik, Rheinbach
Sunrise microplate reader	TECAN, Mondello
Trans-Blot® SD Semi-Dry electrophoretic transfer cell	Bio-Rad, Hercules
Vortex	Labotech, Wiesbaden

3.4. Pearls and Shells

Pearls and shells (fig. 2-3-4) from the Chinese freshwater mussel *Hyriopsis cumingii* (Lea, 1852) (Mollusca, Bivalvia, Unionoida) were bought from different pearl-dealers in Germany and in China. The external calcitic part of the shell was removed using sandpaper in order to expose the nacreous layer. Both samples were accurately cleaned using a 10% solution of sodium hypochlorite and distilled water.

Fig. 2: Chinese cultured pearls from *Hyriopsis cumingii* used in the experiments.

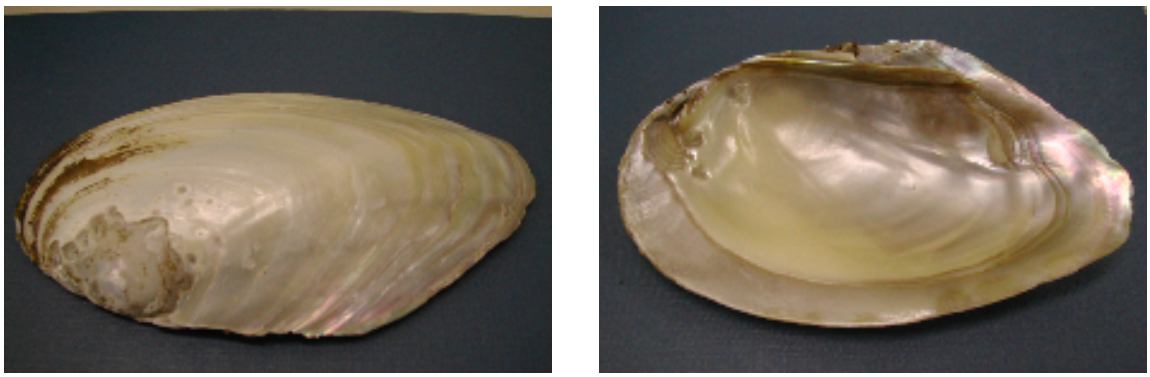

Fig. 3-4: External and internal nacreous layer of the freshwater mussel *Hyriopsis cumingii.*

3.5. Pearls Sections

Thin sections of FWCPs (12 µm thick), were prepared with a diamond-plated saw and polished on a copper plate with diamond paste. Pearl cuts were embedded on a glass slide using a two components epoxy resin (Araldit Rapid) and shortly demineralized with 5% acetic acid.

3.6. Proteins Staining by Coomassie G-250

Proteins present in pearls sections were visualized using Coomassie G-250. This anionic compound creates intensely colored complex with proteins by ionic interactions between its sulfonic acid groups and positive protein amine groups as well as through Van der Waals attractions. Pearls sections were incubated 1 hr in Gel Code Blue Stain Reagent containing Coomassie G-250 and destained in distilled water for 3 hrs. Slides were prepared with glass coverslip and observed under light microscope Olympus.

3.7. PAS Reaction

Periodic Acid Schiff (PAS) reaction was used for demonstration of carbohydrates in pearls sections. Periodic acid (HIO_4) is an oxidizing agent used for converting oxidril groups of 1-2 glycols of pentoses or hexoses in aldehides (fig. 5). Schiff's reagent, a derivate of pararosaniline, interacts with the newly formed aldehydic groups giving a bright pink-purple product. With this method is possible to visualize polysaccharides, mucopolysaccharides, glycoproteins and glycolipids.
The sections previously treated with Coomassie G-250 were incubated in 0.5% periodic acid, 1.5% acetic acid for 1 hour. The slides were extensively washed with distilled water for 1hr and immersed in Fuchsin-sulfite (Schiff's) reagent in the dark for 1 hr. To avoid unspecific reactions the

excess of reagent was washed out with 0.58% potassium metabisulfite in 3% acetic acid. The slides were observed at light microscope

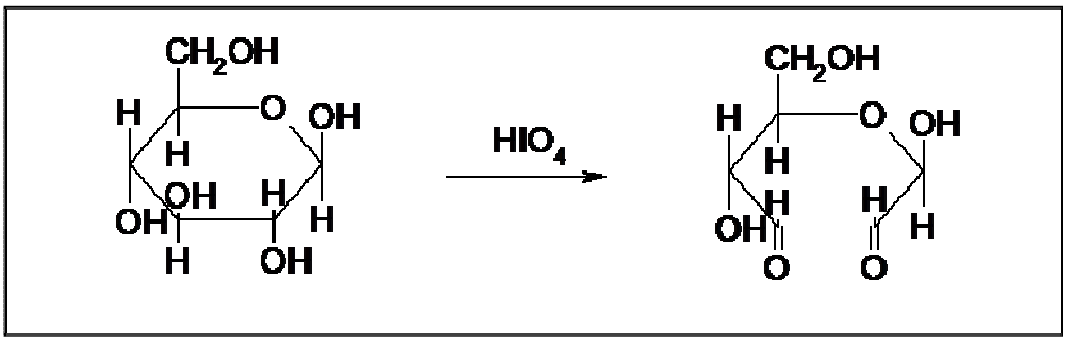

Fig. 5: Oxidation reaction induced by periodic acid: vicinal oxidriles of sugars are converted into aldehydic groups.

3.8. SEM Analysis of Pearls Sections

Fractured and polished pearls cross sections were analyzed under carbon coverage. A Field Emission Scanning Electron Microscopy (FESEM) Leo 1530 coupled with a GEMINI field emission was used to investigate the samples at the micro and nano scale. Secondary electron detector (SED) or a backscattered detector (BSD) was used for the measurements.

3.9. Proteins Extraction

Same quantities of FWCPs and shells were crushed and ground. The obtained powders were placed in SERVAPOR dialysis tubing and sealed with nylon clamps. The membranes were put inside Pyrex test tubes with screw caps, containing a strong acidic ion exchange resin (Dowex 50WX8, H^+ form, 50-100 mesh) suspended in distilled water. This resin is based on a microporous copolymer of

styrene and divinylbenzene in which nuclear sulfonic acid groups are the responsible of the ion exchange. The tubes were gently shaken at +4°C. The demineralization was monitored checking the pH of the suspension. Daily the water was changed and the CO_2 vapours were removed out of the membranes. After complete decalcification, the suspensions were centrifuged (30 min., 5000 rpm, +4°C). The insoluble residues obtained were washed three times with distilled water and stored at -20°C for further analysis. The supernatants were filtered sterile, poured in SERVAPOR dialysis tubing and dialyzed at +4°C against distilled water containing NaN_3 0.001%. After three days the solutions were concentrated with Amicon Ultra-15; these fractions were called soluble extracts.

3.10. Estimation of Protein Concentration (Bradford)

The Bradford dye-binding assay is a colorimetric assay for measuring total protein concentration (Bradford M.M., 1976). This method is based on the binding of Coomassie Brilliant blue to proteins and the consequent shift in absorption of the dye. In order to quantify the protein content in the probes is necessary to use a calibration curve. Protein standards were prepared by serial dilutions of a 2 mg/ml solution of bovine serum albumin (BSA) to final concentrations of 0, 62.5, 125, 250, 500 and 1000 µg/ml. 25 µl of each probe were mixed with 1 ml of Roti-Quant previously diluted 1:5 with distilled water. After 10 min. incubation at RT, 100 µl of each sample were placed in 96-well plate in duplicates and set on the reader. Absorbance was measured at a wavelength of 592 nm. The results were reported in a graph, plotting the value of absorbance at 592 nm vs. protein concentration.

3.11. Extraction of the Residues after Demineralization

The insoluble residues were resuspended in an **extraction buffer** and stirred for 1 hr at room temperature. The samples were centrifuged (12.000 rpm, R.T., 15 min.) and the collected supernatants were prepared for electophoretic analysis using ReadyPrep 2-D Cleanup Kit.

Extraction buffer

1.6% NP40 , 150 mM NaCl , 0.25% Sodium dodecyl sulphate (SDS) ,0.1% Deoxycholic acid (DOC), 50 mM Tris pH 8.8

3.12. SDS-Polyacrylamide Gel Electrophoresis (SDS-PAGE)

SDS-PAGE has is a widely used technique used for many common lab procedure; as establishment of protein size, protein identification, determination of sample purity, identification of disulfide bonds, quantification of proteins and blotting applications. The protein sample is preliminary mixed and boiled with a loading buffer containing SDS and β-mercaptoethanol; these compounds are denaturing agents, which at 95 °C cleave proteins by reduction of disulfide bonds: the only known covalent bond between the polypeptide chains. Thus proteins will be unfolded into the primary structure. SDS is contained in the loading dye, in the gel and in the running buffer, it is an anionic detergent that binds quantitatively to proteins, giving them all an equal negative charge. The so treated proteins probes are ready to be loaded in the polyacrylamide gel. Polyacrylamide is a linear polymer that can be cross-linked with N, N'-methylene-bis-acrylamide giving a gel matrix with controlled pore size. According the application of the polyacrilamide gel, the concentration of these two compounds can be varied. In this study we used a 40% solution (Rothiphorese 40 29:1) containing 38.67% (w/v) of acrylamide and 1.33% (w/v) of bis-acrylamide. Polymerization of the gel was initiated by free radicals, generated by ammonium persulfate (APS) activated in presence of a catalyst as N, N, N', N'-tetramethylethylenediamine (TEMED). The ratio between acrylamide/bis-acrylamide and the final concentration of the mixture, regulate the dimension of the pores in the gel and consequently the resolution of separation process. When an electric field is

applied, proteins negatively charged migrate to the anode; having all an equal charge and a linear structure, their motility depends exclusively on the molecular weight. The migration distance during the electrophoresis is then linearly dependent on the logarithm of the molecular size (Weber K. and Osborn M., 1969). Using protein standards of known molecular weight is possible to evaluate the mass of the probes.

In a discontinuous system a stacking gel is layered on top of a resolving gel having higher pH and a different ionic strength. This allows the proteins to be concentrated into a tight band in the upper gel before entering the lower one and to produce a gel with tighter and better separated bands. Minigels (7 cm x 8 cm x 0.75 or 1 mm) having a concentration of 12 or 15% in the lower part and overlaid with an 8 % stacking gel were prepared according Tab.1 and 2. The gels were used directly or stored after casting in humid conditions at 4°C. PAGE was carried in vertical electrophoresis tanks (Mini Protean II) following the procedure of Laemmli (Laemmli U.K., 1970). Non-denaturing conditions were also used, omitting β-mercaptoethanol and the heating step (tab. 3). By comparison of not denaturing gels with denaturing ones is possible to identify eventual polymeric structures, detect monomers and other subunits.

STACKING GEL	
Rothiphorese Gel 40%	8%

RESOLVING GEL	
Tris HCl pH 8.8	0.375 M
Rothiphorese Gel 40%	15-12%
Glycerol	2%
SDS	0.1%

APS	0.1%
TEMED	0.01%

Tris HCl pH6.8	0.250 M
Glycerol	2%
SDS	0.1%
APS	0.1%
TEMED	0.01%

Tab. 1-2: Composition of the upper and the lower SDS gel.

	I	II
Tris HCl pH 6.8	62.5 M	62.5 M
Glycerol	10%	10%
SDS	2%	2%
Bromophenol blue	0.002%	0.002%
β-mercaptoethanol	5%	--

Tab. 3: Composition of loading buffer for denaturing (I) and not denaturing (II) gels.

Running buffer:

- 25 mM Tris
- 192 mM Glycin
- 0.1% SDS

pH 8.3

3.13. Semi-Native PAGE

In a semi-native gel electrophoresis the interactions of the subunits within a multimeric protein are generally retained by omission of β-mercaptoethanol and the heating step. SDS is not present in the loading and running buffer, while its concentration in the gel is decreased to 0.01% (Tab. 4, 5 and 6). This procedure maintains the polypeptides in an original conformation and gives information about the quaternary structure of a protein.

STACKING GEL	
Rothiphorese Gel 40%	8%
Tris HCl pH6.8	0.250 M
Glycerol	2%
SDS	0.01%
APS	0.1%
TEMED	0.01%

RESOLVING GEL	
Rothiphorese Gel 40%	12%
Tris HCl pH8.8	0.375 M
Glycerol	2%
SDS	0.01%
APS	0.1%
TEMED	0.01%

Tab. 4-5: Composition of a discontinuous SDS gel under semi-native conditions

Tris HCl pH 6.8	12.5 M
Glycerol	10%
Bromophenol blue	0.001%

Tab. 6: Composition of loading buffer for gel under semi native conditions.

Running buffer for semi-native gels:

- 25 mM Tris
- 192 mM Glycin

pH 8.3

3.14. Coomassie Staining with Gel Code Blue Stain Reagent

Gel Code Blue Stain Reagent utilizes the colloidal properties of Coomassie G-250 for protein staining on polyacrylamide gels; the detection is fast and highly sensitive. After electrophoresis, gels were washed twice with distilled water with gentle shaking for 15 min. For an 8 x 10 cm mini gel, 20 ml of GelCode Blue Stain Reagent were used. Stain intensity reached a maximum within approximately 1 h. After staining, gels were washed with distilled water until no background was visible. Fixation of low molecular proteins was enhanced by washing the gels directly after SDS-PAGE with 10% methanol, 7% acetic acid for 30 min.
Gels were acquired using Odyssey infrared Imaging System.

3.15. Fixation and Silver Staining (Gotliv B.-A., 2003)

Switzer *et al.* in 1979 developed the silver stain technique as a very sensitive method for protein visualization in SDS slab gels with a detection level in a range between 0.3 and 10 ng (Switzer R.C., 1979). The mechanism of reaction is based on the binding of silver ions to the amino acid side chains, mainly to the sulfhydryl and carboxyl groups of protein, followed by reduction to free metallic silver. A modification of this classic method was made by Gotliv *et al*. in order to visualize acidic proteins extracted from mollusc shells generally poorly stained with classis methods. The gel after electrophoresis was incubated 1 hr in 50% methanol, 18% formaldehyde, 12% acetic acid, and then the solution was replaced with 10% glutaraldehyde. After 30 minutes the gel was washed three times (20 min. each) with 50% ethanol, thus the procedure reported in the manual of the Bio-Rad Silver Stain Kit was followed.

3.16. Protein Purification

The 48 kDa protein from pearls soluble extract was purified by cutting the corresponding band obtained after SDS-PAGE separation. The piece of gel was placed inside the glass tubes of the Electro-Eluter System filled with running buffer having same composition of the one used for SDS-PAGE. Electroelution was carried applying 8-10 mA per tube under continuous stirring. After 6 hrs the buffer in the tank was replaced with fresh running buffer prepared without SDS. After 1 hr proteins were completely eluted from the polyacrylamide gel and recovered in solution. Purity and concentration of the eluted protein were checked with SDS-PAGE.

3.17. Polyclonal Antibodies Production

Polyclonal antibodies (PoAb) were raised against the purified 48 kDa pearls protein by immunization in female rabbits (White New Zealand) as described (Harlow E., 1988). PoAb are derived from different B-cell lines. They are a mixture of immunoglobulin molecules secreted against a specific antigen, each recognizing a different epitope. Injection of antigen into the rabbit induces the B-lymphocytes to produce IgG immunoglobulins specific for the antigen. 10 µg per each injection of the protein purified as previously described, were diluted in phosphate-buffered-saline (PBS) containing Freund's adjuvant (complete and incomplete). After three boosts the serum was collected; the PoAb was termed *PoAb-glycoPearl48*. The specificity of the produced antibodies was checked by Western Blot.

3.18. Western Blot against PoAb-glycoPearl48

Reactivity against *PoAb-glycoPearl48* of soluble and insoluble extracts from pearls and shells was checked by Western Blot. After SDS-PAGE separation, proteins were transferred at 40 mA for 90 min using a semi-dry transfer cell TRANS-BLOT SD, on a PVDF membrane previously activated in methanol and then incubated for 30 min in transfer buffer. After electrophoresis the membrane was blocked overnight at +4°C in 1% blocking solution in TBS. Then the membrane was washed three times in TBS-T, and incubated for 1 hr with *PoAb-glycoPearl48* (1:20000) prepared in 0.5% blocking solution. After the washing step with TBS-T, the membrane was incubated for 1 hr in a solution (1:5000) of anti-rabbit IgG alkaline phosphatase conjugate from goat in 0.5% blocking solution. The immunocomplexes were visualized with the color develop system NBT/BCIP. As control, immunoblotting against pre-immune serum was performed using the same procedure.

Transfer buffer:

- 25 mM Tris
- 192 mM Glycin
- 20% Methanol (v/v)

pH 8.3

Blocking solution:

- 1% Western Blocking Reagent (Roche) in TBS (v/v)

TBS:

- 10 mM Tris-HCl
- 150 mM NaCl

pH 8,0

TBST:

- 0.1% Tween 20 in TBS (v/v)

Detection buffer (P3):

- 100 mM Tris-HCl
- 100 mM NaCl

pH 9.5

NBT (nitrotetrazolium blue chloride) solution:

- 75 mg/ml NBT in 70 % N,N-Dimethylformamide (v/v)

BCIP (5-bromo-4-chloro-3-indolyl phosphate disodium salt) solution:

- 50 mg/ml BCIP in 100 % N, N-Dimethylformamide (v/v)

3.19. Isoelectric Focusing and Second-Dimensional Electrophoresis

Isoelectric focusing (IEF) is used to separate proteins according to their charge and to determine the isoelectric point (pI). pI is the value of pH at which a polypeptide subjected to an electric field and in presence of amphoteric molecules (ampholytes), reaches a net charge of zero, and stops to migrate. The resulting pI is determined by the number of acidic and basic residues present in the polypeptide and is a peculiar characteristic of each protein. At physiological pH, the carboxyl groups of acidic residues are predominantly deprotonated and impart a negative charge. In contrast, the amine groups of basic residues are protonated and generate a positive charge. To perform IEF the sample is loaded onto a gel strip, in which a pH gradient is established, thus an electric current is applied; in this conditions negatively charged proteins will move towards the anode, while positive ones will migrate to the cathode. The protein is "focused" when stops in the zone in which its charge is zero. Following the horizontal isoelectric focusing, a proteins mixture can be further separated according the molecular weight in a second dimension by SDS-PAGE. This technique, known as two dimensional gel electrophoresis (2-D PAGE), is used to study post-translational modifications (phosphorilation, glycosilation, etc...) that affect the charge of a protein more than the molecular weight. This two-dimensional separation according pI and mass allows resolution of polypeptides that would not normally be clearly separated by a one-dimensional method.

The samples containing 20 μg of proteins were prepared using ReadyPrep 2-D Cleanup Kit and resuspended in **rehydration buffer**, then loaded on the strips (ReadyStrip IPG Strip, pH 4/7, 7cm)

and rehydrated under passive condition for 16 hours in PROTEIN IEF Cell. The absorbed proteins were focused in an automated run at +22^{o}C, 10 000 V-hr. After IEF, IPG strips were equilibrated in **equilibration buffer** containing 1% DTT for 15 min and then further incubated in the same buffer for another 20 min replacing DTT with 1.5% iodoacetamide. After equilibration, the IPG strips were placed on the top of a 12% SDS-polyacrilamide gels and sealed with 0.1% agarose supplemented with bromophenol blue. SDS-PAGE was run at 100 V for 15 min as initial migration and increased to 150 V for separation. 2-D SDS-PAGE standards were used as marker. Gels were stained in GelCode Blue Stain Reagent and imaged with Odyssey infrared Imaging System. Western Blot against *PoAb-glycoPearl48* was also performed as previously described.

Rehydratation Buffer:

- 8 M urea
- 0.2% ampholytes 4/7
- 60 Mm DTT
- 0.001% bromophenol blue

Equilibration Buffer:

- 6 M urea
- 2% SDS
- 30% glycerol
- 50 mM Tris-HCl

pH 8.8

3.20. Glycoproteins Detection by Lectin (Hsi K.-L., 1991; Bédouet L., 2001)

Lectins are proteins that form reversible complexes with mono- and oligo-saccharides. Wheat germ agglutinin (WGA) from *Triticum vulgaris* was used for identification of glycoproteins in the soluble extracts. In order to amplify the intensity of the signal a system biotin-avidin was applied. WGA was used in conjugation with biotin; this water soluble vitamin binds with high specificity avidin, a

glycoprotein present in egg white. Each avidin molecule can link 4 biotins, this multiple interaction results in an enhancement of the signal. After separation with SDS-PAGE the polypeptides were transferred to the PVDF membrane by semi-dry transfer procedure. The membrane was saturated with **blocking solution** for 1hr, with gentle shacking at R.T. Blocking solution was replaced by Lectin from *Triticum vulgaris* biotin conjugate solution in a final concentration of 2 µg/ml and incubate 2 hrs in the same conditions. The membrane was washed three times for 10 min with **washing buffer**, and immersed in avidin-alkaline phosphatase diluted 1:5000 in Tris 50mM pH 7.5. The glycoproteins were visualized using as substrate an NBT/BCIP solution in **P3 buffer**. Precision Plus Protein Standards Dual Color and fetuin (1µg) were included in the gel as molecular weight marker and positive control.

Blocking solution

- 2% polyvinylpirrolidone
- 0.5 M NaCl
- 50mM Tris-HCl

pH 7.5

Washing buffer

- 0.1 % Triton X-100
- 0.5 M NaCl
- 50 mM Tris

pH 7.5

P3 buffer

- 100mM Tris
- 100mM NaCl

pH 9.5

3.21. Enzymatic Deglycosilation

Proteins contained in the soluble extracts, were enzymatically deglycosilated using Enzymatic CarboRelease Kit according to the recommended protocol and testing the reaction by SDS-PAGE, as previously described. Fetuin was used as positive control.

The Enzymatic CarboRelease Kit removes all N-linked oligosaccharides and many O-linked oligosaccharides from glycoproteins. N-links (Asn-linked) are removed using the enzyme *PNGase F*. In addition all Ser/Thr-linked (O-linked) Gal-(β1-3)-GalNAc-(α1) and all sialic acid substituted Gal-(β1-3)-GalNAc-(α1) will be removed using the combination of *sialidase* and *O-glycosidase*. The addition of *β-galactosidase* and *hexosaminidase* will assist in the deglycosilation of larger O-link structures.

3.22. Stains-All

The cationic carbocyanine dye Stains-All ((1-ethyl-2- [3-(1-ethyl-naphthol[1,2-d]thiazolin-2-ylidene)-2- methylpropenyl]naphthol[1,2-d]thiazolium bromide), interacts with different proteins giving specific colored dye-protein complexes. Has been shown (Golberg H.A., 1997; Campbell K.P., 1983) that sialoglycoproteins, phosphoproteins, acidic and calcium binding proteins, interact with the dye, shifting the adsorption spectrum. The resulting complexes are blue, while almost all other macromolecules give red color. After SDS-PAGE, the gel loaded with the extracts form shells and pearls, was rinsed in 25% isopropanol for three times and incubated for 10 min in the same solution. This procedure was repeated for three times; therefore the gel was shook for 3 hrs in the dark in **Stains-All** solution. Bands were revealed washing extensively with 25% isopropanol.

Stains-All solution:

- 0.025% Stains-All
- 30 mM Tris
- 7.5% formamide
- 25% isopropanol

pH 8.8

3.23. Immunostaining of Demineralized Pearls and Shells

Immunochemistry allows the identification of proteins expressed in a biological sample using a specific reaction antigen-antibody. This staining technique is widely used in diagnostics and in laboratory research for understanding the distribution and localization of proteins in different parts of a tissue.

The organic matrix was exposed by demineralization, and labeled using PoAb-*glycoPearl48*. Pearls and shells pieces were demineralized in a solution 1 M EDTA pH 8, 4% formaldehyde. After 48 hrs, samples were extensively washed in distilled water for 30 min. The organic matrix was separated by peeling and placed on glass slides previously treated with polylysine. Slides were incubated O.N. in blocking solution (4% BSA in PBS) at +4°C, then washed three times (10 min. each) with PBST. *PoAb-glycoPearl48* diluted 1:500 in PBS was added to each sample. After 1 hr slides were washed with PBST and incubated for 1 hrs in the dark with anti-rabbit IgG Cy3 conjugated antibody diluted 1:2000 in PBS at R.T. After washing, the fluorescence analysis was performed with an Olympus AHBT3 light microscope together with an AH3-RFC reflected light fluorescence attachment at emission wavelength 546 nm.

3.24. Immunogold Labelling of Pearls

In order to visualize the protein using a Scanning Electron Microscope, the specific secondary antibody, is conjugated with gold nanoparticles. Silver enhancement was used in order to increase the dimension of gold particles.

In this study, immunogold labelling was used to localize the soluble protein in the calcium carbonate structures. Small pieces of FWCPs were shortly etched in 10 mM acetic acid (pH 3.5). After 1 minute the samples were washed in 10 mM $NaHCO_3$ (pH 9.5) and then in distilled water. The pieces were blocked O.N. in 4% BSA in PBS, at +4°C, then washed three times with PBS containing 0.1% Tween-20 (PBS-T) and incubated for 2 hrs at R.T. in *PoAb-glycoPearl48* diluted 1:200 in 2% BSA in PBS. After three PBS-T washing, samples were incubated for 2 hrs in the dark in anti-rabbit IgG Gold antibody diluted 1:20 in 2% BSA in PBS at R.T. After three washes in PBS-T followed by as many in PBS. The pieces were rinsed in distilled water and treated with Silver Enhancer Kit. Samples were dried and covered with carbon for SEM visualization.

3.25. Carbonic Anhydrase (CA) Activity Detection

Carbonic anhydrase activity in the samples was tested using an established assay (Armstrong J.M, 1966). This assay is based on the esterase activity of carbonic anhydrase and the specific inhibition of *acetazolamide*. After enzymatic cleavage of the ester bond of *p*-nitrophenylacetate, the production of the yellow compound *p*-nitrophenol was monitored using a spectrophotometer (fig.6).

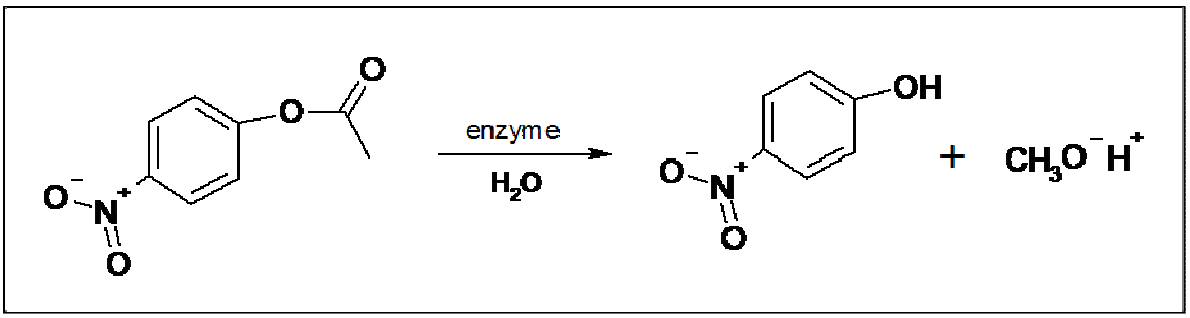

Fig. 6: Enzymatic esterase reaction of p-nitrophenylacetate. After hydrolysis nitrophenol and acetic acid are formed.

The reaction was initiated mixing in a 96 Assay Plate 66 µl of the substrate *p*-nitrophenylacetate 0.03 M with 134 µl of a Tris solution (pH 7.4) containing the soluble extracts in various concentrations. The enzymatic activity was monitored reading with Titertek Multiskan Plus the increase in absorbance at 405 nm during the time (30 min.). The blank was prepared using only the substrate in Tris buffer. As negative and positive control, bovine serum albumin (BSA) and carbonic anhydrase (CA) from bovine erythrocytes were used. For inhibition studies *acetazolamide* in a final concentration of 0.1 mM was added.

3.26. Protein Labelling with FITC

Fluorescein isothiocyanate (FITC) (fig. 7) is a fluorophore derived of fluorescein and is the simplest and most commonly used reagent for labelling proteins. It has a molecular weight of 389 Da, excitation and emission wavelengths at 494 nm and 520 nm, respectively. The isothiocyanate group is responsible of the crosslink with amino, sulfhydryl, imidazol, tyrosyl or carbonyl groups on a protein; however only primary and secondary amines yield stable products.

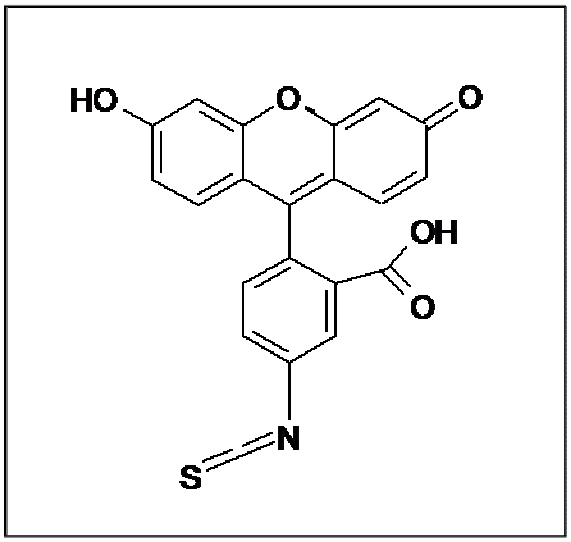

Fig. 7: Structure of FITC. The isothiocyanate group links to the proteins by covalent bonds

100 µl of the protein sample having a concentration of 0.66 mg/ml were dialyzed for 1 hr against 50 mM borate buffer, pH 8.5 at room temperature, using a dialysis unit (3,5 kDa MWCO) with float. The solution was transferred in a tube and mixed with 0.9 µl of FITC 0.1 mg/ml in dimethylformamide (DMF). After 1hr incubation in the dark, the mixture was dialyzed again PBS in order to remove the excess of the fluorescent reagent.
Pearls soluble extract coupled with FITC was used in the precipitation assay as further illustrated.

3.27. Calcium Carbonate Precipitation

Calcium carbonate crystals were formed using a common method in which gaseous CO_2 is mixed with a $CaCl_2$ in dH_2O. The reaction was carried in a hermetically sealed desiccator and ammonium carbonate $(NH_4)_2CO_3$ was used as source of CO_2 (fig. 8).
Lab-Tek Chamber Slide Systems containing $CaCl_2$ 1 mM, supplemented with several concentration of pearls and shells extracts, pearls extract coupled with FITC or BSA, were exposed to the vapour

of ammonium carbonate in a desiccator at R.T., for different times (2, 24 and 48 hrs). Controls were prepared without any protein addition.

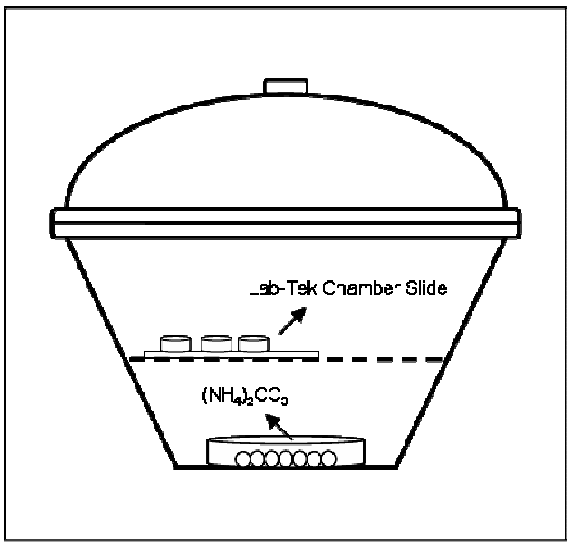

Fig. 8: Scheme of desiccator. Ammonium carbonate in placed in the lower compartment. CO_2 vapours released enter in the chamber slides containing different reaction solutions.

3.28. Calcium Carbonate Precipitation with PoAb-glycoPearl48

$CaCO_3$ precipitation was conducted as previously described, in presence of the soluble pearls extract preliminary incubated for 10 minutes in a 1:1000 solution of *PoAb-glycoPearl48* in distilled water. Controls were performed using only polyclonal antibodies.

3.29. Calcium Carbonate Precipitation with Acetazolamide

The same precipitation assay was performed using 1 mM Acetazolamide in controls and in presence of pearls and shell extracts.

3.30. Crystals Analysis and Characterization

After precipitation, the crystals obtained were washed extensively with distilled water and dried. Crystals were analyzed with optical microscope, Scanning Electron Microscopy (SEM), confocal microscope, Scanning Transmission Electron Microscopy (STEM), High Resolution Transmission Electron Microscopy (HRTEM), Electron Diffraction (ED) and Raman Spectroscopy.

3.31. Raman Spectroscopy

When electromagnetic radiation passes through matter, the most of them continues along the original directions but a small fraction is deviated in others. Light that is scattered due mainly to vibrations in molecules of a solid is called Raman scattering. The difference in energy between the incident photon and the Raman scattered photon is equal to the vibrational energy of the molecule. Raman spectrum is obtained plotting the intensity of scattered light versus energy difference. Raman Spectroscopy is a non-destructive method with several applications in chemistry, diagnostic, polymer analysis, pharmacology, mineralogy and crystallography (McCreery R.L., 2001; Spiro T.G., 1988; Mahadevan-Jansen A., 1996; Wartewing S., 2005). In this study Raman Spectroscopy was used for an identification of $CaCO_3$ polymorphs. All Raman spectra were recorded at room temperature using a Horiba Jobin Yvon LabRAM CCD-detector (Peltier-cooled), an integrated Olympus BX41 optical microscope and an x-y-stage automatically controlled by software and a joystick. A 100x long-distance objective was selected. The reflected light and Rayleigh light were

reduced using the respective notch filters. The 531.21 nm line of a laser was used for excitation. A grating with 1800 grooves per mm and a silt width of 100 μm were chosen and the laser power was 10 mW.

3.32. Scanning Transmission Electron Microscopy (STEM), High Resolution Transmission Electron Microscopy (HRTEM) and Electron Diffraction (ED)

Transmission Electron Microscopy was performed by a Tecnai F30, equipped with a field emission gun electron source and an accelerating current of 300kV. Scanning Transmission Electron Microscopy (STEM) images were collected by a FISCHIONE dark field detector that allows a big contrast even in low dose conditions. High Resolution Transmission Electron Microscopy (HRTEM) images were collected with a 14-bit GATAN 794MSC CCD and allow a theoretical resolution of 1.5 Angstrom.

Electron Diffraction (ED) was collected by the same GATAN CCD. During ED analysis, high energy electrons are scattered by atoms giving a specific diffraction pattern. The resulting pattern gives information about the investigated structure in form of rings (for amorphous or poly-crystalline materials) or single spots (for single crystals). Calculation of the interplanar distances allows a specific characterization of crystals; electron diffraction pattern gives also important information about symmetry, lattice parameters and crystals orientation.

Vaterite crystals obtained in the previously described precipitation assay were initially visualized using Scanning Transmission Electron Microscopy (STEM) and High Resolution Transmission Electron Microscopy (HRTEM) and then subjected to Electron Diffraction (ED).

3.33. Confocal Laser Scanning Microscopy

The main technical difference between a confocal microscope and a conventional optical one is the presence of two pinholes in the light axis. This results in a limitation of the illumination field eliminating any light scattering and increasing effective resolution. The image captured in this way is relative only to the fluorescence of the section focused. Pictures of consecutive sections can be assembled to obtain high resolution 3D images. The analysis of crystals obtained with pearls extract FITC conjugated was performed using a Leica DMIRE2 inverted microscope connected to LEICA CTRMIC electronic box; images were acquired by means of LEICA Confocal Software.

3.34. Immunostaining of the Crystals

Immunostaining was used to detect the soluble proteins on the surface of the $CaCO_3$ crystals formed during the precipitation assay.

Crystals were blocked O.N. in blocking solution (4% BSA in PBS) at +4°C, then washed three times (10 min. each) with PBS and incubated for 2 hrs at R.T. in *PoAb-glycoPearl48* diluted 1:200 in PBS. After washing, crystals were incubated for 2 hrs in the dark in anti-rabbit IgG Cy3 conjugated antibody diluted 1:2000 in PBS at R.T. After washing, the fluorescence analysis was performed with an Olympus AHBT3 light microscope together with an AH3-RFC reflected light fluorescence attachment at emission wavelength 546 nm.

3.35. Crystals Dissolution

Calcium carbonate crystals precipitated in presence of pearls soluble proteins as previously described, were divided in two aliquots and treated as following: one was directly dissolved in acetic acid 3%, while the other part was incubated for 10 minutes with a solution containing urea

4M and SDS 2% in order to remove the proteins on the surface. After several washes with distilled H_2O, crystals were solubilized in acetic acid 3%. Each probe was mixed with reducing sample buffer and applied to SDS-PAGE for WB analysis against *PoAb-glycoPearl48*.

3.36. Precipitation on Control Calcite Crystals

Rhombohedral calcite crystals were obtained using a solution 10 mM $CaCl_2$. The slides containing the crystals were subjected to further precipitations in presence of pearls soluble extract and the FITC conjugated one. Controls were performed without protein addition.

4. RESULTS

4.1. Pearls Sections Staining and SEM Analysis

The reaction with Coomassie G-250 of the organic matrix resulted in a strong blue coloration of the polypeptides previously exposed by acidic demineralization. Schiff's reagent evidenced with a wide purple staining that a large part of the organic matrix is represented by polysaccharides (fig. 9). The same slides clearly showed also the organization of the proteins in concentric layers, in which, as pointed out in SEM pictures, the inorganic phase is included as aragonite tablets (approx. 5-10 µm in diameter and 200-500 nm thick), arranged in a typical "*brick and mortar*" structure (fig. 10).

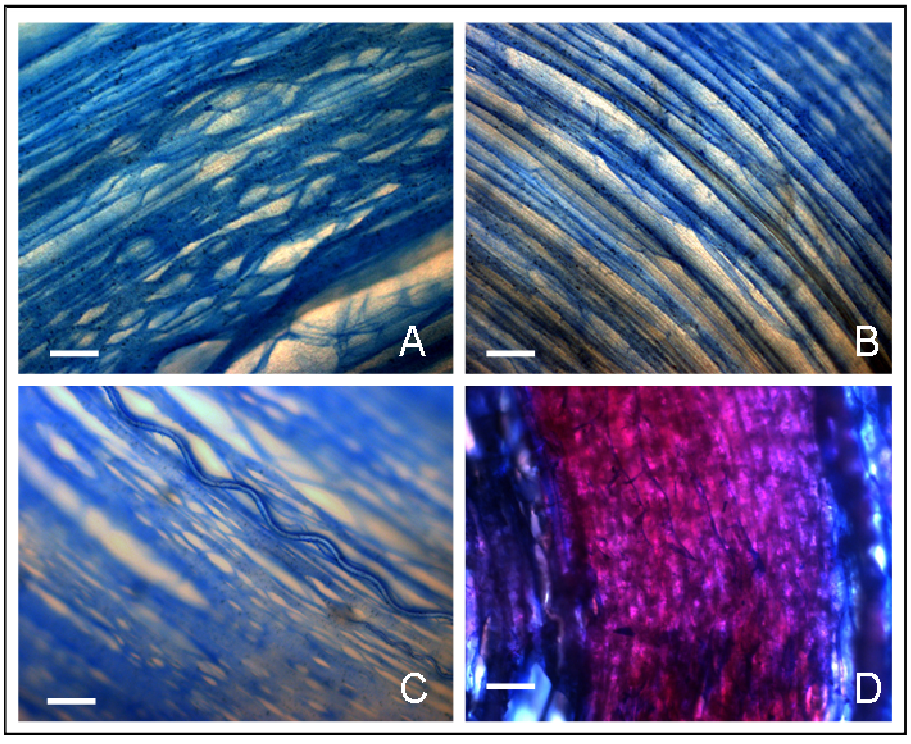

Fig. 9: (A, B, C) Longitudinal FWCP sections stained with Coomassie G-250. Proteins were stained in blue; the disposition of the organic components in concentric layers was clearly highlighted. In D the same section treated with Coomassie was stained also with Schiff's reagent. The wide purple coloration indicates a high content of polysaccharides. (Scale Bar: 10 µm)

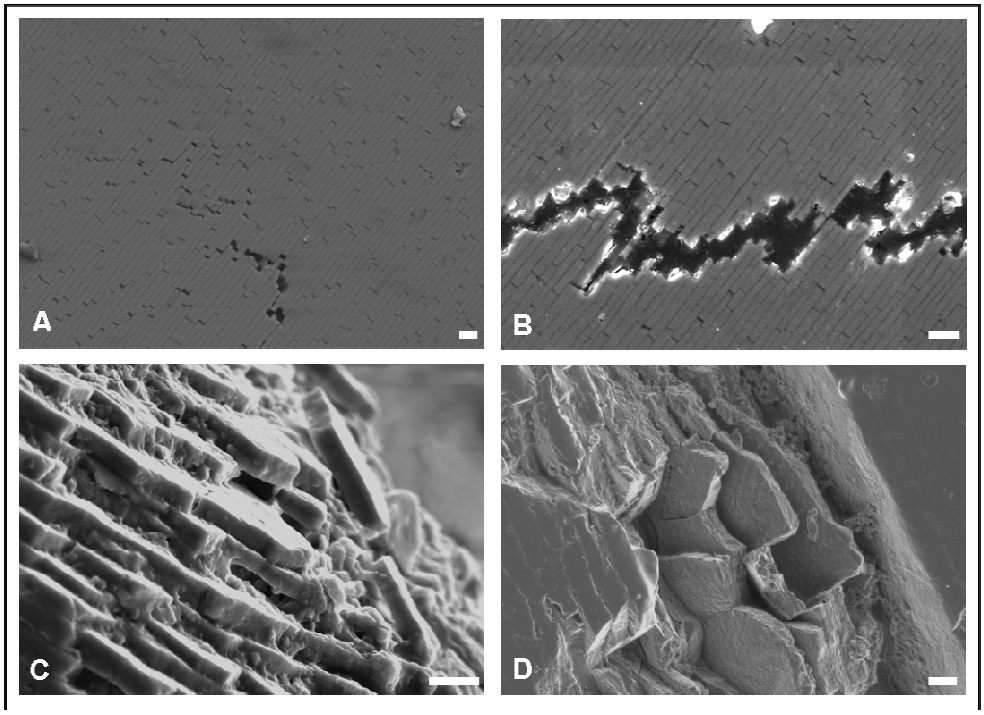

Fig. 10: SEM pictures of FWCP sections. In A and B aragonite tablets are neatly arranged as bricks in a wall. Higher magnifications (B, D) evidence the organic matrix intimately associated with the aragonite platelets. (Scale Bar: 1 μm)

4.2. Proteins Extraction and Electrophoresis Analysis

After demineralization of the FWCPs and shell powders, a soluble fraction and an insoluble one were obtained. Using SDS-PAGE under reducing conditions, the former fraction revealed two main bands for each extract. Specifically, pearls extract gave a band at 48 kDa and one at 24 kDa, while the shell extract showed bands at 44 kDa and 22 kDa. Using non reducing and seminative conditions the lower molecular bands disappeared and only the 44 kDa band for shell was displayed. In pearls sample a higher band having about 100 kDa size was revealed together with the one at 48 kDa (fig. 11).

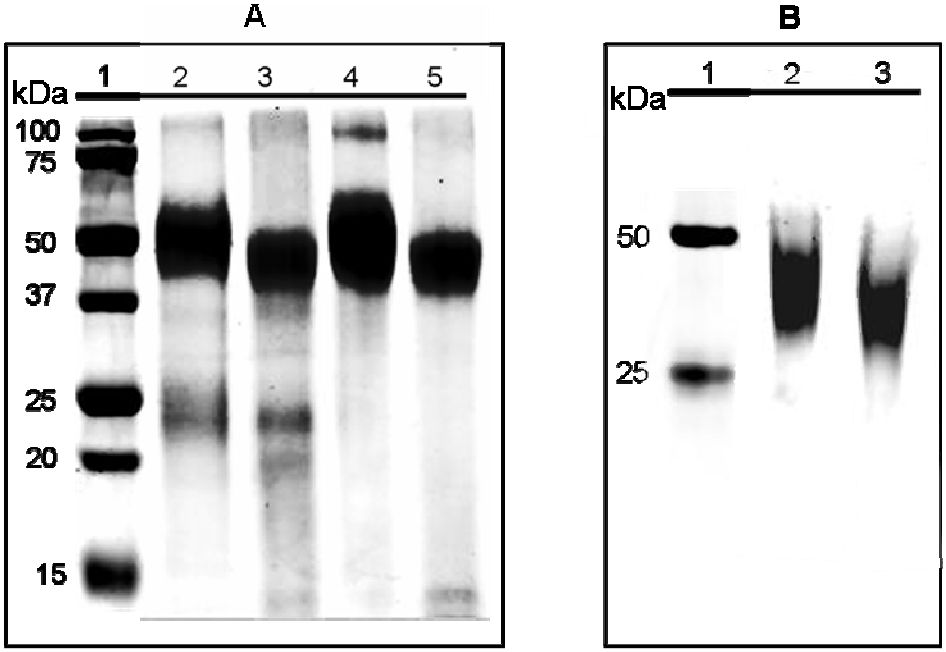

Fig. 11: (A) 12% SDS PAGE: 1) DualColor Protein Standards, 2-3) pearls and shell soluble extracts under reducing conditions, 4-5) pearls and shell extracts under not reducing conditions. **(B)** Semi native PAGE: 1) Protein Standard, 2) pearls extract, 3) shell extract.

4.3. Coomassie and Silver Staining: Comparison

The protein pattern obtained after Coomassie staining of polyacrilamide gel is not so different from the one treated with fixative and visualized using Silver reagent (fig. 12).

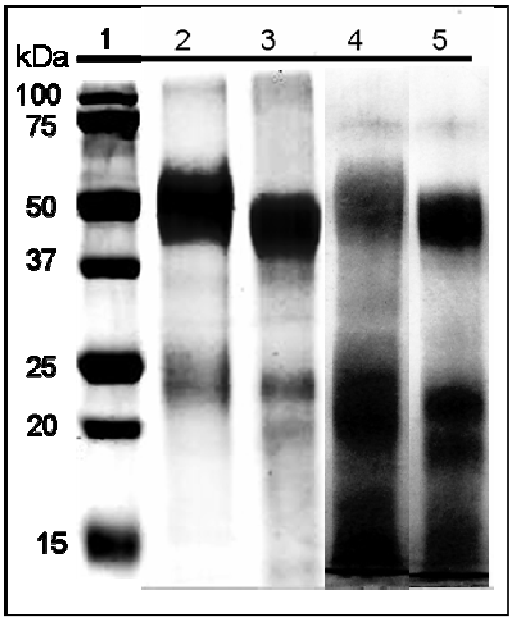

Fig. 12: 12% SDS PAGE: 1) DualColor Protein Standards, pearls and shell soluble extracts under reducing conditions stained with Coomassie (2-3), and Silver Stain Kit after preliminary fixation (4-5).

4.4. Insoluble Residues Analysis

After complete extraction of the insoluble residue, SDS-PAGE analysis revealed for both extracts an equal single band relative to a protein having a molecular weight of approximately 13 kDa. When beta-mercaptoethanol and the heating step were omitted the same polypeptides were detected at higher molecular weight values due to their non linear conformation and no additional bands were noticed (fig. 13).

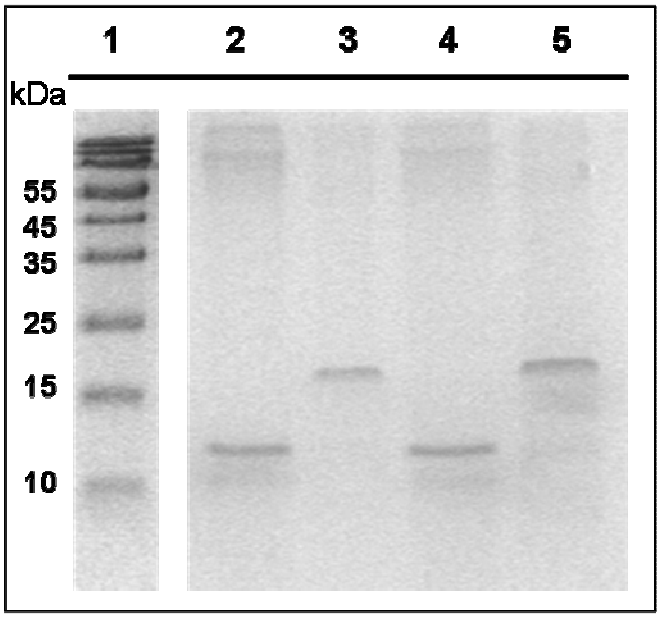

Fig. 13: 15% SDS PAGE of the insoluble residues: pearls (2-3) and shell (3-4) extracts respectively under reducing and without denaturating agents. Lane 1: PeqGOLD Protein Marker I.

4.5. Western Blot against PoAb-glycoPearl48

Polyclonal antibodies raised against the pearl-48kDa-protein gave the same strong reaction for the soluble extracts from shells and pearls (fig. 14). No reaction was reported for the insoluble extracts (data not shown).

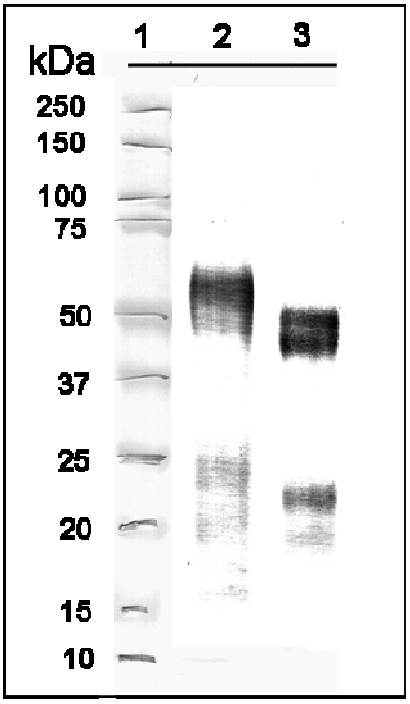

Fig. 14: WB of the shell (2) and pearls (3) soluble extracts vs. *PoAb-glycoPearl48*. (1) DualColor Protein Standards.

4.6. Second-Dimensional Gel Electrophoresis

Coomassie staining and WB of the second-dimensional electrophoresis gel indicated an acidic isoelectric point of the protein extracts. By comparison of the patterns obtained, was possible to notice a number of post-translational modifications for the 48 kDa pearls protein higher than for the 44 kDa one from shells (fig. 15).

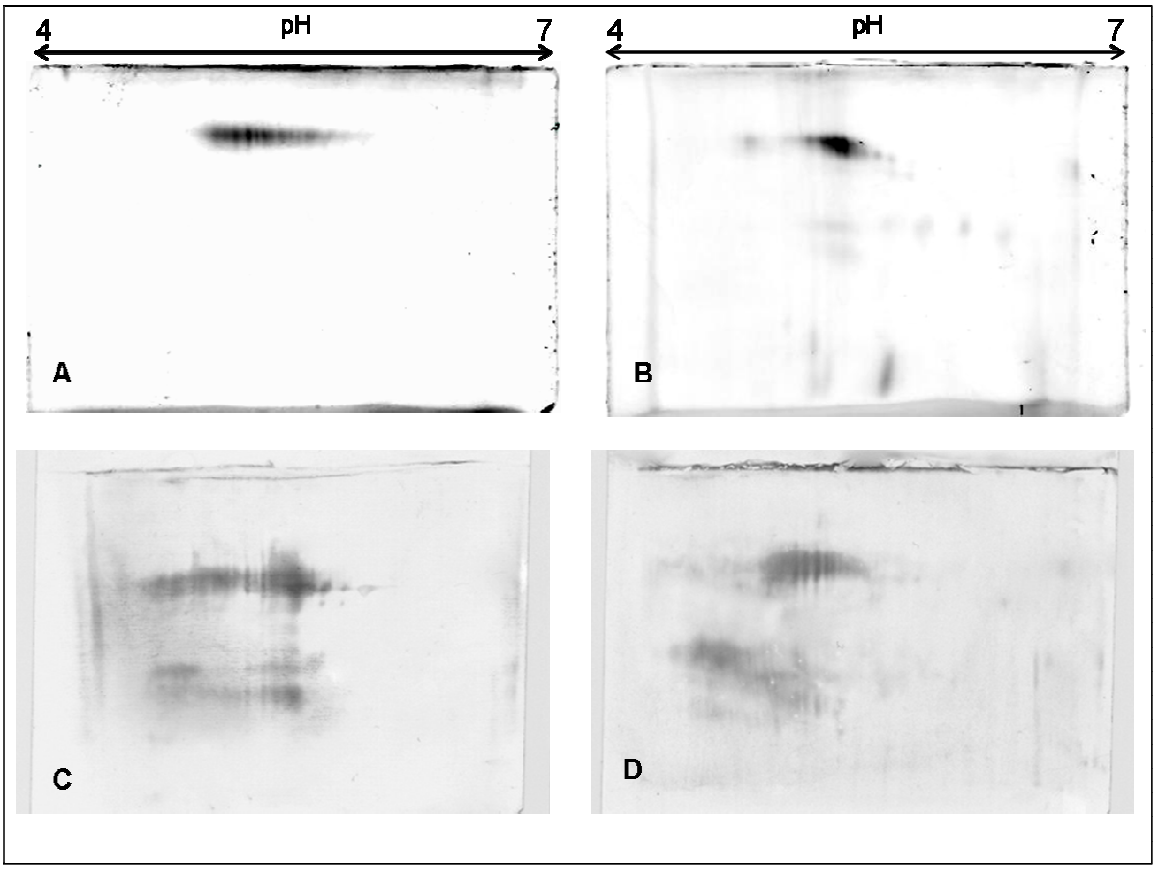

Fig. 15: 2D gels stained using GelCode Blue Stain Reagent of pearls (A) and shell (B) soluble extracts. Under are reported the corresponding WB against *PoAb-glycoPearl48* for pearls (C) and shell (D) probes.

4.7. Glycosilation Studies

Lectin recognition gave a positive reaction for both extracts (fig. 16). As well the enzymatic deglycosilation succeeded and was verified by the formation of lower molecular weight bands in SDS gels, due to the loss of the sugar groups (fig. 17).

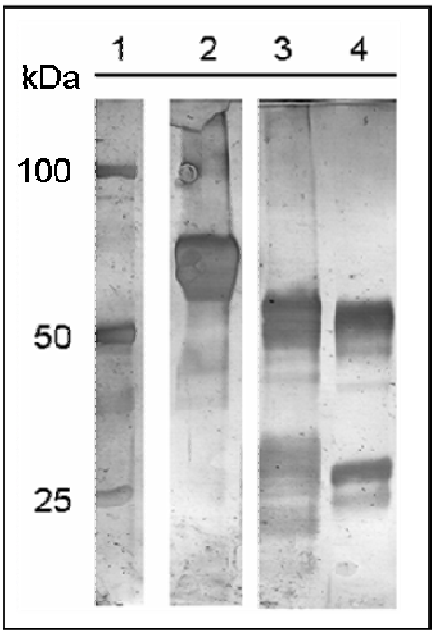

Fig. 16: Detection of carbohydrates by biotinylated wheat germ agglutinin. 1) Dual Color molecular weight marker, 2) fetuin, 3-4) pearls and shell soluble extracts.

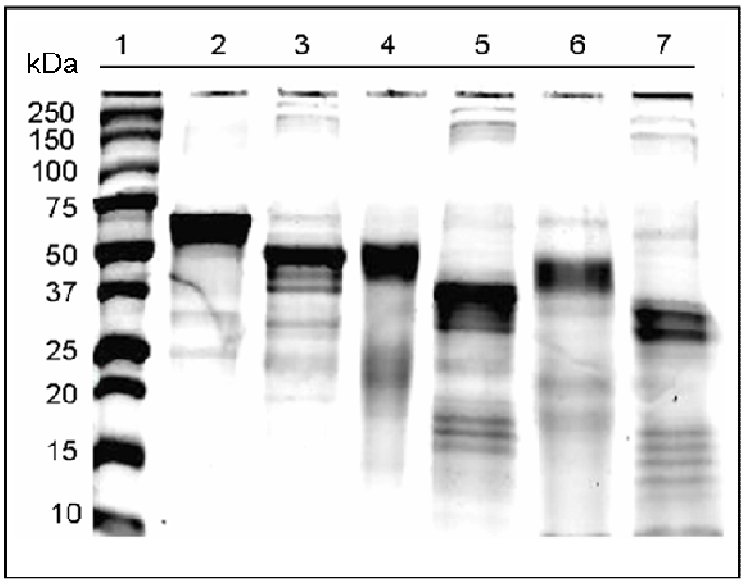

Fig. 17: 12% SDS PAGE before and after enzymatic deglycosilation. Lane 2 untreated fetuin, lane 3 fetuin after deglycosilation. Lanes 4 and 6: untreated extracts from pearls and shell. Lanes 5 and 7 deglycosilated extracts from pearls and shells. Lane 1 Dual Color molecular weight marker.

4.8. Stains All

Incubation of SDS-PAGE gel with the cationic carbocyanine dye (Stains-all) resulted in a blue coloration of the 48 kDa and 44 kDa bands respectively for pearls and shells extract (fig. 18).

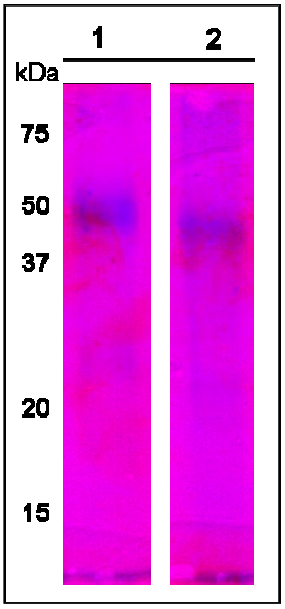

Fig. 18: 12% SDS PAGE of pearls (1) and shell (2) soluble extracts stained with Stains All. On the left molecular weight markers are reported.

4.9. Immunostaining of Demineralized Pearls and Shells

The specific immune reaction described the soluble glycoproteins in the intertabular matrix surrounding aragonite tablets. Images show hexagonal structures in which calcium carbonate was located. Their diameter is slightly bigger in shells than in pearls (fig. 19).

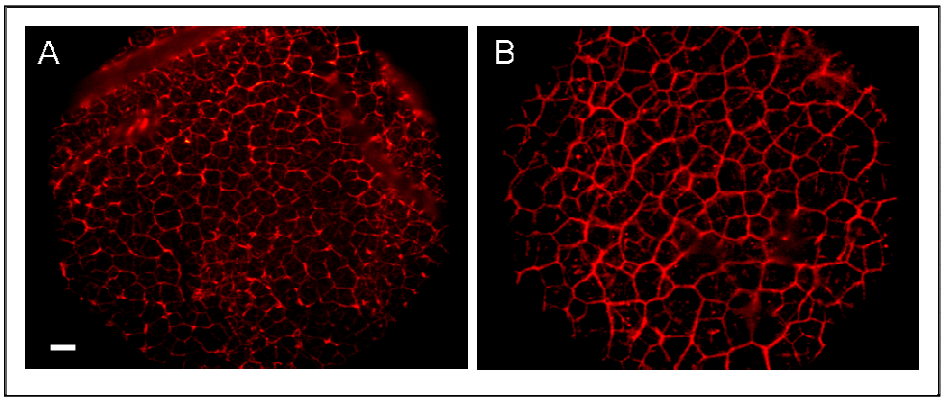

Fig. 19: Immunostaining of pearls (A) and shells (B) demineralized nacre. The net-like structure is composed by the intertabular matrix surrounding each aragonite tablet (Scale Bar: 5µm).

4.10. Immunogold Labelling of Pearls

Immunolocalization showed clearly the wide distribution of the soluble proteins in shells microstructures and inside the nacre. The polypeptides are present together with the organic sheet on the surface of the calcium carbonate tablets and also between the inorganic layers as part of the interlamellar matrix (fig.20a). Higher magnification images describe the polypeptide as main component of the organic bridges between different calcium carbonate layers (fig.20b).

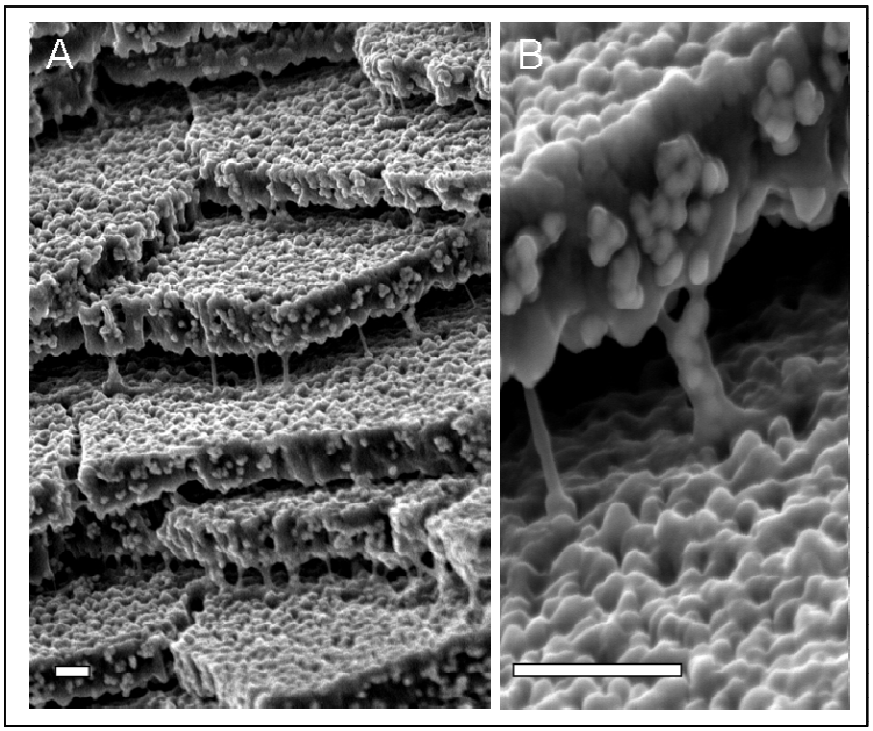

Fig. 20: Scanning Electron Microscope images of a pearl subjected to immunogold labelling using the *PoAb-glycoPearl48***.** White globular structures indicate gold nanoparticles associated to the secondary antibody. The soluble protein in widely expressed on the surface of calcium carbonate platelets as showed in A. In B higher magnification allows to individuate the same protein in the inter-lamellar matrix as constituent of the organic bridges between the inorganic layers **(**Scale Bar: 200 nanometers).

4.11. Carbonic Anhydrase Activity

The protein extracts from shell and pearls showed both similar enzymatic activities. In a concentration of 20 µg/ml the extracts accelerated the rate of the hydrolysis of *p*-nitrophenylacetate. Their catalytic activity was totally inhibited by addiction of acetazolamide, as for carbonic anhydrase in the positive controls. No activity was registered using the same concentration of BSA (fig. 21).

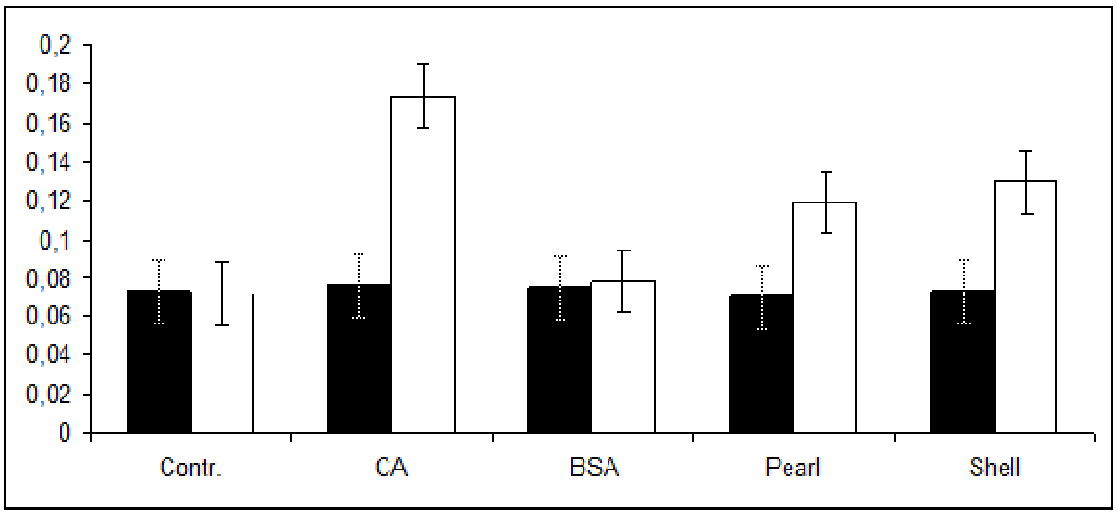

Fig. 21: Hydrolysis of p-nitrophenyl acetate. The reaction was monitored reporting in the black columns the increase in absorbance at 405 nm during 30 min. BSA, pearls and shell soluble extracts were added in final concentration of 20 µg/ml, as positive control carbonic anhydrase (CA) 5 µg/ml was used. In the white columns, effect of acetazolamide 0.1 mM.

4.12. Calcium Carbonate Precipitation, SEM and Raman Analysis

Calcium carbonate precipitation conducted in controls using only $CaCl_2$ 1 mM gave rhombohedral calcite crystals, having regular and smooth surface, same results were obtained adding BSA 10 µg/ml. In presence of 10 µg/ml soluble extract from shell, small calcite crystals with irregular shapes were precipitated, while when the 48 kDa glycoprotein obtained from pearls was added, almost only flat rounded crystals were detectable (fig. 22). Raman Spectroscopy identified these crystals as vaterite while the calcium carbonate obtained in the other conditions was calcite (fig. 23). No differences were registered when the incubation time was increased from 2 hrs to 24 or 48 hrs. When the pearls extract was incubated with PoAb-glycoPe48, the effect on crystal morphology was totally inhibited, while in presence of acetazolamide no effects were noticed (data not shown).

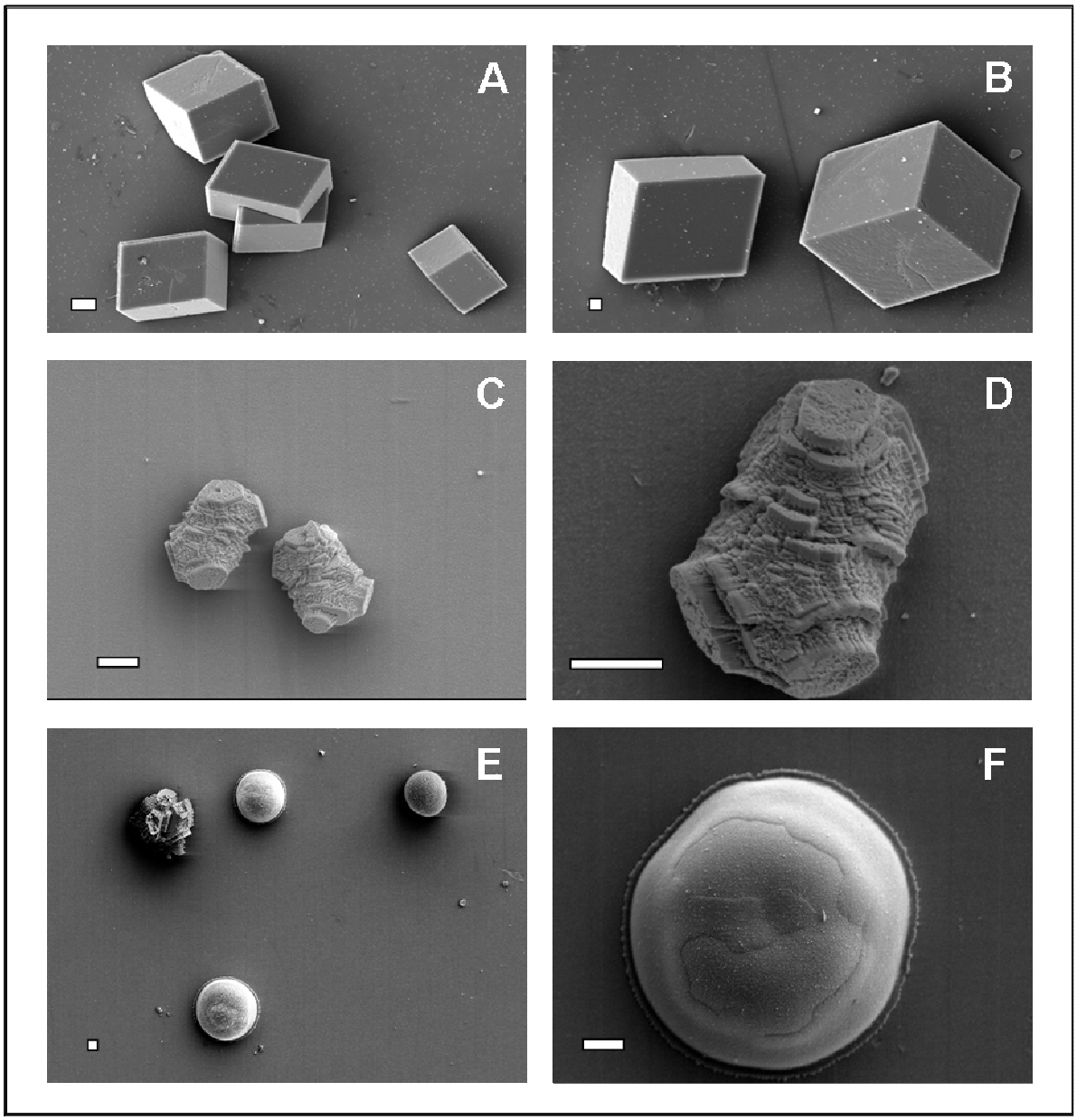

Fig. 22: SEM pictures of calcite crystals obtained in control (A) and in presence of BSA 10 µg/ml (B). In C calcium carbonate crystal precipitated using shell soluble extract. 5000x magnification of the previous sample. When the pearls extract was added mainly rounded crystals were obtained as showed in pictures E and F (Scale Bar 5µm).

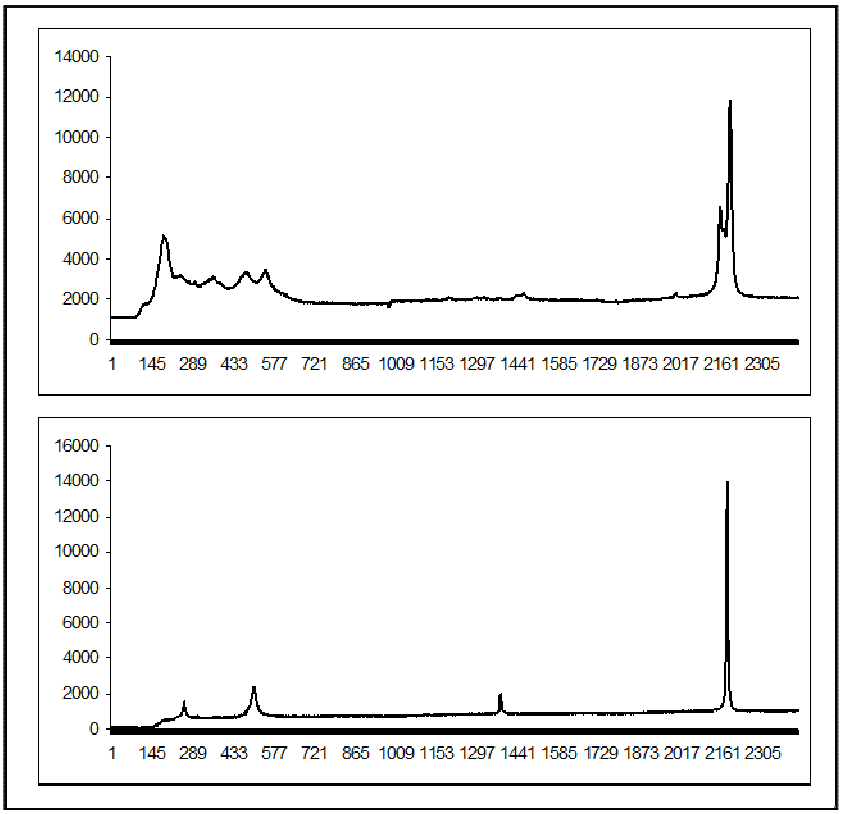

Fig. 23: (Up) Raman spectrum for calcite registered in controls and samples containing BSA or shell extract. **(Down)** Raman spectrum of vaterite for crystals precipitated with pearls extract. Intensity (arbitrary units) vs. wavenumber cm $^{-1}$ are reported on the axis.

4.13. ED, STEM and HRTEM

The STEM images evidenced a discontinuous growth of the vaterite particles, characterized by concentric rings structure (fig. 24a). The external ring mainly consists of acicular crystals with radial elongation. The big particle is then surrounded by small spheres of vaterite 10-30 nm in diameter. HRTEM images of the same particle show that the particle is formed by many small domains having diameter less than 1 micron and different orientations (fig. 24b). ED confirmed the poly-crystallinity of the particle (fig. 24d). The interplanar distances relative to the round crystals identified as vaterite after Raman Spectroscopy are: 1.8; 2.1; 2.7; 3.3 and 3.6 Angstrom. Comparison of these results with the data found in literature confirmed to be crystalline vaterite. (Kamhi S. R., 1963; Downs R. T., 1993; McConnel, J.D.C., 1960; Anthony J. W., 2001-2005).

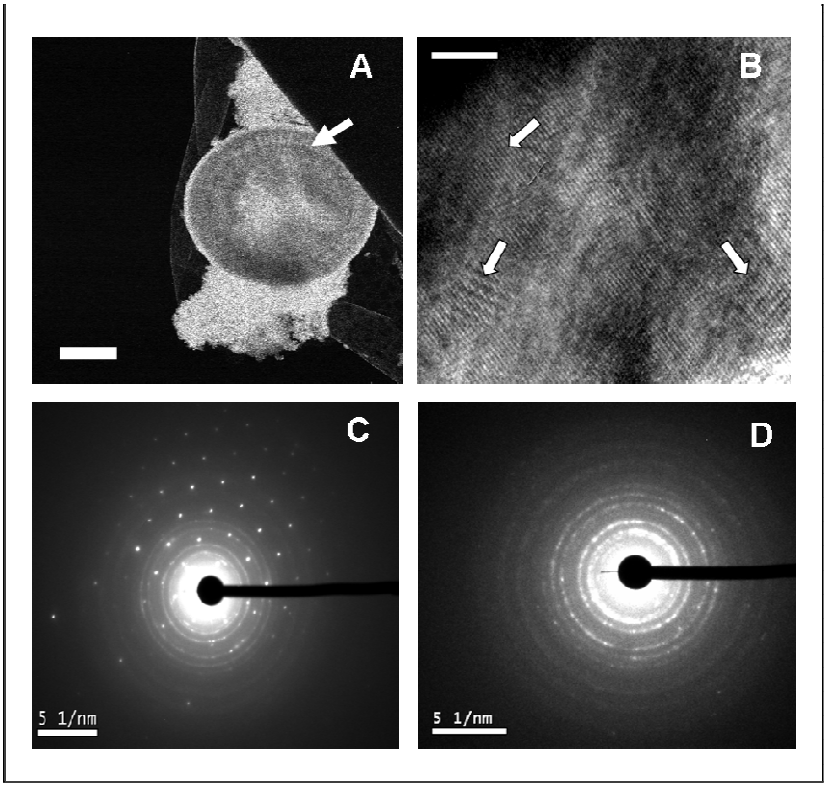

Fig. 24: (A) STEM image of vaterite, the arrow shows a clear discontinuity in growth (Scale Bar: 2µm). In B: HRTEM picture of the same crystal. Arrows indicate domains with different orientations (Scale Bar: 5 nm). Down: simultaneous diffraction of a single calcite crystal (C) and a poly-crystalline vaterite particle. The difference in cell parameters is evident.

4.14. Crystals Dissolution

The membrane subjected to WB against PoAb-glycoPe48 revealed the bands corresponding to the pearls extract either in the crystals directly dissolved either in the ones previously washed with urea-SDS (fig. 25).

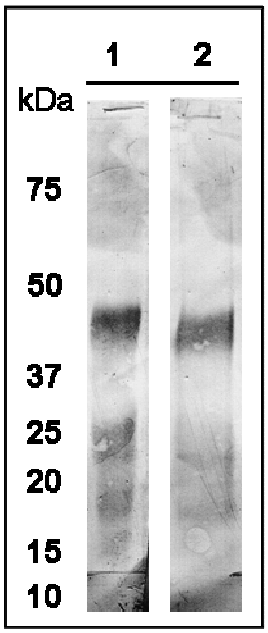

Fig. 25: Western Blot vs. PoAb-glycoPe48 of the crystals directly dissolved (1) and after cleaning with urea-SDS solution (2). On the left molecular weight standards were reported.

4.15. Immunostaining of the Crystals

Immunostaining using *PoAb-glycoPe48* localized the soluble protein from pearls and shells on the surface of the precipitated crystals (fig 26c and 26d). No reaction occurred for controls and crystals obtained in presence of BSA (fig. 26a and 26b).

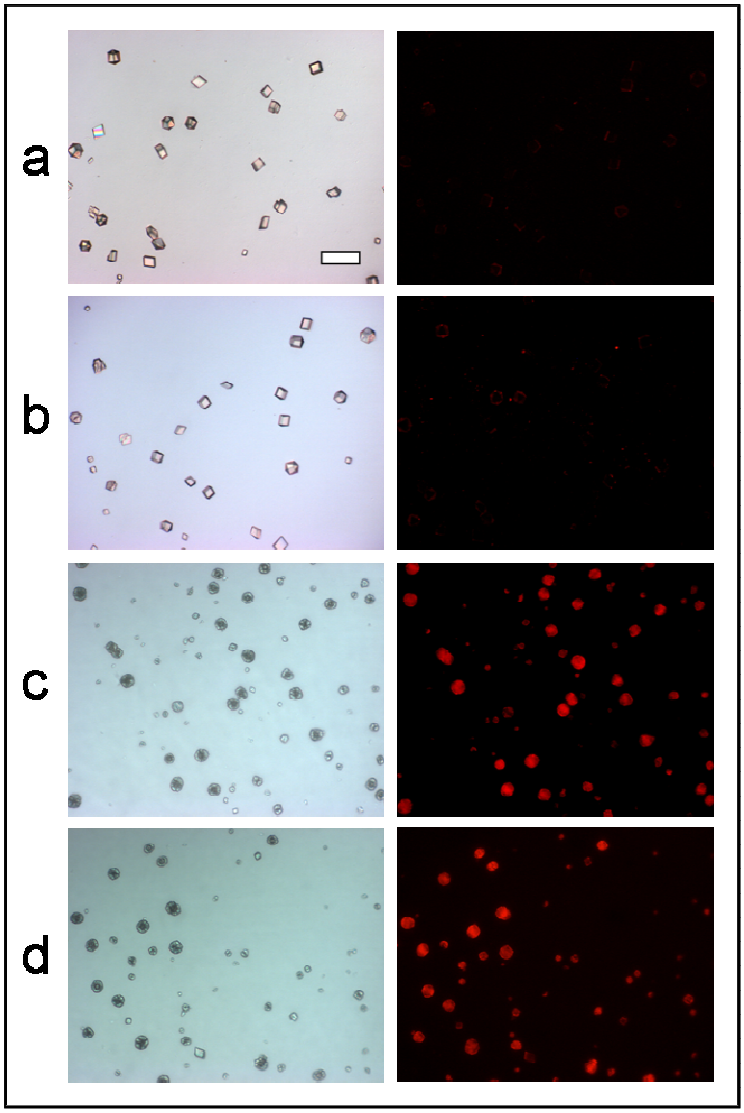

Fig. 26: Light (left) and fluorescence (right) microscopic images of the crystals subjected to immunostaining. In the first line (A) calcium carbonate crystals obtained in controls. (B) Crystals precipitated in presence of BSA. High fluorescence was showed in crystals obtained adding pearls (C) and shells (D) soluble extracts. (Scale Bar: 50 µm)

4.16. Precipitation Using FITC Labelled Extract

Microscopic images of the crystals obtained adding the FITC coupled protein, described this protein intimately associated with the precipitated calcium carbonate (fig. 27), but the exact localization of the protein is not clear. Confocal Laser Scanning Microscopy analysis allowed a clear visualization also inside the crystal. The resolution of the instrument gave several sections 300 nm thick from the top to the bottom of the sample. The resulting fluorescence indicated the pearls soluble protein both on the surface and inside the crystal (fig. 28). Fig. 29 shows an inner section of vaterite in which is more evident the presence of the protein in the central nucleation point of the crystal.

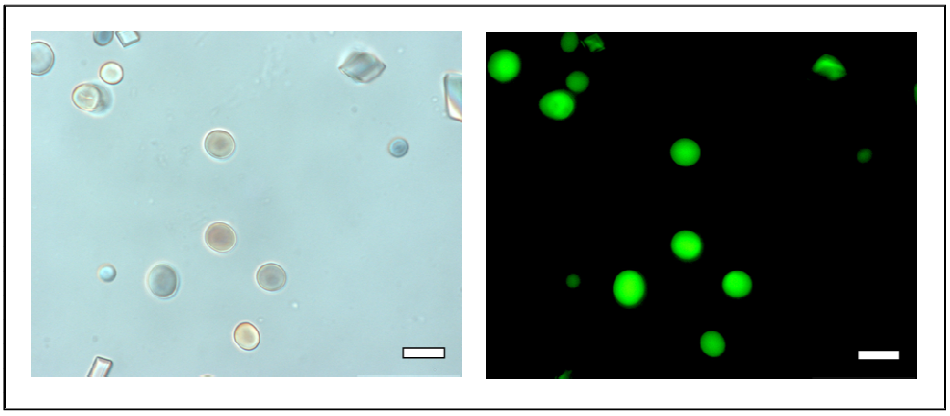

Fig. 27: Light and fluorescence microscope images of vaterite crystals containing protein extract from pearls conjugated with FITC. Scale Bar 20 µm.

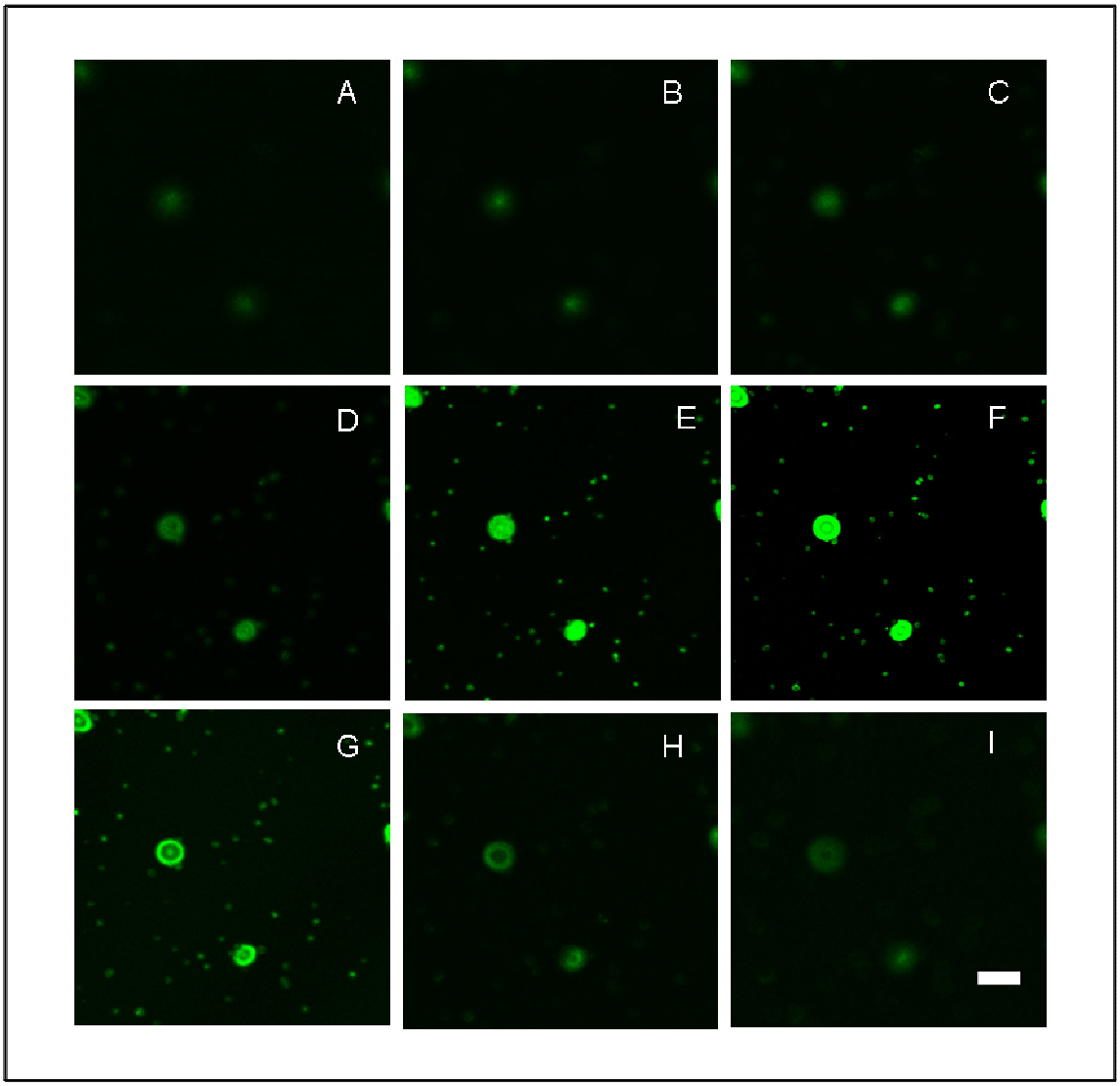

Fig. 28: Confocal laser microscope images of 300 nm thick sections of calcium carbonate crystals (from the top to the bottom) obtained in presence of protein soluble extract from pearls conjugated with FITC. Scale Bar 50 µm.

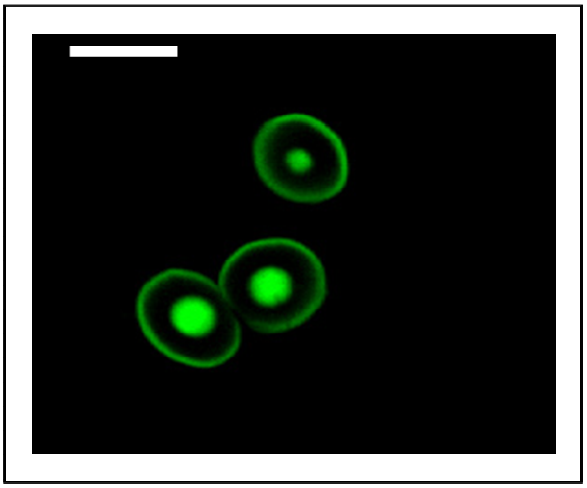

Fig. 29: Internal section of a **v**aterite observed under confocal microscope. Proteins are localized both in the inner part and on the surface of the crystal. Bar 20 μm.

4.17. Precipitation on Control Calcite Crystals

When repeated precipitations were performed on control calcite using pearls extract, overlapped layers were formed onto the surface of the starting crystals (fig.30), while sporadic or no additional apposition of mineral was observed in controls and in presence of BSA (data not shown). These new formed layers were easily detected when FITC coupled extract was used (fig. 31).

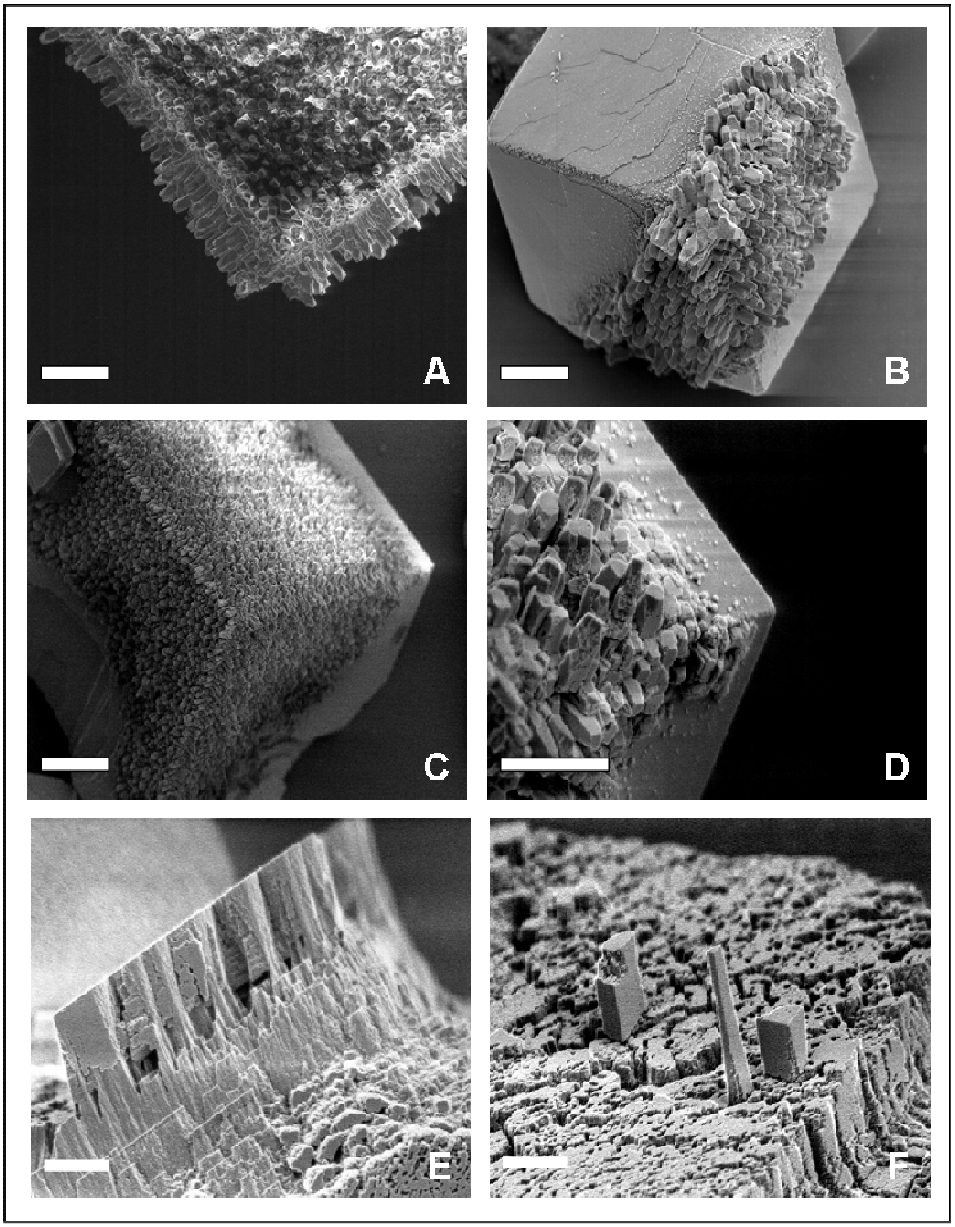

Fig. 30: A, B, C and D: SEM pictures of calcite rhombohedral crystals subjected to a single calcium carbonate precipitation in presence of pearls soluble extract. Additional crystals grew on the regular calcite surface. In E and F magnification of new calcium carbonate formations, when several precipitations were performed. Scale Bar 20 μm.

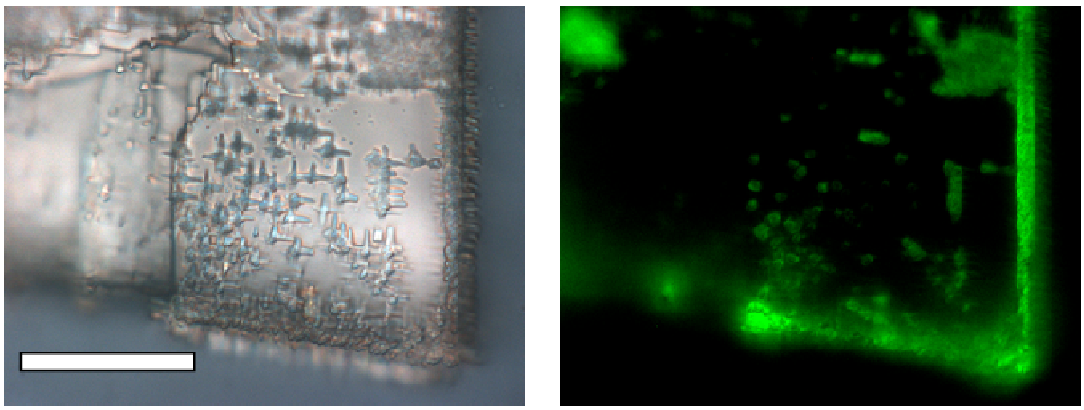

Fig. 31: Light and fluorescent microscope images of calcite control crystals subjected to calcium carbonate precipitation in presence of pearls extract FITC- conjugated.

5. DISCUSSION

For the first time the protein content from shells and pearls of the same animal were analyzed and compared, proposing also their role in biomineralization processes. The freshwater mussel *Hyriopsis cumingii* was chosen for this study because it is the most used in Chinese cultured pearls production, and because no artificial nuclei are introduced as trigger, so that the resulting pearls don't contain any extraneous material. In some recent papers (Qiao L., 2007; Wehrmeister U., 2007; Ma H.J., 2006), pearls obtained from this animal, showed an elevated content of vaterite. The unusual presence of this high energetic and rare polymorph of calcium carbonate is quite surprising and it is also related to the final quality of such pearls. In the preliminary microscopic analysis, shells and pearls revealed a hierarchical and ordered "brick and mortar" structure common to almost all biominerals containing calcium carbonate. The inorganic component composed of aragonite tablets is associated with the organic matrix that in pearls is disposed in concentric layers in which a large part is represented by polysaccharides.

In order to obtain the organic matrix a preliminary demineralization was necessary. The most common protocols use in this step acetic acid or ethylenediaminetetraacetic acid (EDTA). We avoided both reagents due to the possible degradation of the proteins by acetic acid and the interference of EDTA in the following precipitation assay. For these reasons a styrene-divinylbenzene resin, having sulfonic acid as functional groups was chosen. This resin allowed decalcification by ion exchange, without interference with the samples. After shells and pearls demineralization, the attention was focused on the soluble fractions, especially on two polymeric proteins with similar molecular weight. In order to obtain a complete proteins pattern a modified silver staining protocol was used (Gotliv B.A., 2003). This technique requires a preliminary strong fixation, in order to avoid the small acidic polypeptides to migrate out the gel. The results were compared to the ones obtained using Coomassie G-250 and no significant differences were noticed. The first evidence was that these polypeptides, extracted only after dissolution of calcium carbonate, are intimately associated with the inorganic phase. The similar reactivity of both extracts in immumoblotting against the *PoAb-glycoPe48*, suggested

that the two polypeptides are the same, but the one obtained from pearls is characterized by a slightly higher molecular weight. The reason of this difference was explained by two dimensional gel electrophoresis; in fact the resulting patterns showed that the pearls protein has a larger number of spots indicating a higher degree of post-translational modifications. Reaction with Lectin and enzymatic deglycosilation, shown that these modifications were sugar groups, as confirmed also from the strong reaction of pearls sections using PAS staining. The 2D analysis indicated moreover an acidic isoelectric point of the polypeptides, also verified by using Stains All. This method revealed a blue coloration of the corresponding bands characteristic for highly acidic and potential Ca^{2+} binding proteins (Golberg H.A., 1997; Campbell K.P., 1983; Sharma Y., 1989). These results focused our attention on the extracted glycoproteins as potential tools for biomineralization processes; in fact several publications already described how acidic, calcium binding and glycosilated proteins extracted from shell nacre, act as specific regulators in calcium carbonate precipitation (tab.7) (Addadi L., 1985; Gotliv B.A., 2003; Marin F., 2008). The importance of the soluble peptide was further evidenced using immunogold labelling technique. SEM images described this protein as one of the main components of the organic sheet surrounding the calcium carbonate tablets. The same protein is as well localized in the intertubular and in the interlamellar matrix, taking part in the formation of the organic bridges that glue vicinal mineral layers. Brocken tablets indicated the glycoprotein also inside of the inorganic structures. Another interesting feature of these soluble proteins was found in their carbonic anhydrase activity. Carbonic anhydrase is an essential metalloenzyme that regulates many physiological functions in mussel tissues, as respiration processes and pH regulation. Its activity is based on the catalysis of the reversible hydration of CO_2, according the following reaction:

$$H_2O + CO_2 \leftrightarrow HCO_3^- + H^+$$

So generated bicarbonate (HCO_3^-) and the deriving carbonate (CO_3^{2-}) anions are able to interact with Ca^{++} ions and enhance precipitation by supersaturation of $CaCO_3$ in the extrapallial fluid present between the mantle and the shell. This mechanism suggests an important role of the enzyme also in biomineralization processes (Wilbur K.M., 1955; Miyamoto H., 1996; Yu Z., 2006).

PROTEIN	ORIGIN	CHARACTERISTICS	REF.
Freshwater organisms			
Dermatopontin (19.6 kDa)	*Biomphakaria glabrata* *	Glycosilated	Marxen J.C., 1997
P95 (95 kDa), P50 (50kDa), P29 (29 kDa)	*Unio pictorium*°	Acidic, glycosilated, Ca^{++} binding	Marie B., 2007
Marine organisms			
AP24 (24 kDa)	*Haliotis rufescens**	Acidic, Ca^{++} binding, glycosilated	Michenfelder M., 2003
AP7 (7kDa)	*Haliotis rufescens**	Acidic, Ca^{++} binding	Michenfelder M., 2003
AP8 (8 kDa)	*Haliotis rufescens**	Acidic, Ca^{++} binding	Fu G., 2005
Lustrin A (142 kDa)	*Haliotis laevigata** (shells and pearls)	Ca^{++} binding, CA activity, glycosilated, Component of the adhesive between aragonite tablets	Shen X., 1997
MSI60	*Pinctada fucata*°	Ca^{++} binding, acidic	Sudo S., 1997
Mucoperlin (66.7 kDa)	*Pinna nobilis*°	Glycosilated, acidic, Ca^{++} binding, $CaCO_3$ ppt inhibition	Marin F., 2000
N14 (13.7 kDa)	*Pinctada maxima*°	Acidic	Kono M., 2000
N66 (59.8 kDa)	*Pinctada maxima*°	CA domain, similar to nacrein	Kono M., 2000
Nacrein (60 kDa)	*Pinctada fucata*°	CA activity, Ca^{++} binding, $CaCO_3$ ppt inhibition	Miyamoto H., 1996
P14 (14.5 kDa)	*Pinctada fucata*°	Induces aragonite ppt	Ma C., 2005
Pearlin (15 kDa)	*Pinctada fucata*° (pearls)	Mucopolysaccharide, acidic, Ca^{++} binding, belongs to N16 family (Samata,1999)	Miyashita T., 2000
Perlucin (17 kDa)	*Haliotis laevigata**	$CaCO_3$ ppt promotion, glycosilated	Weiss I.M., 2000
Perlustrin (13 kDa)	*Haliotis laevigata**	Similar to lustrin A	Weiss I.M., 2000
Perlwapin (18 kDa)	*Haliotis laevigata**	$CaCO_3$ ppt inhibition, acidic	Treccani L., 2006

Tab.7: Principal nacre-associated proteins from gastropods (*) and bivalves (°). Acidic proteins are meant those having a pI < 6. (CA: Carbonic Anhydrase, $CaCO_3$ ppt: calcium carbonate precipitation).

Nacrein and other nacrein-related proteins such as N66, contain a carbonic anhydrase-like domain, and are the major component of the soluble organic matrix of several marine mollusks. It was well described that these proteins by concentration of bicarbonate ions can regulate the nucleation and the morphology of calcium carbonate crystals *in vitro*, showing their fundamental effect in shell formation. (Norizuki M., 2008; Miyamoto H., 2005).The hypothesis upon the involvement of shell and pearls soluble glycoproteins in biomineralization was confirmed by means of $CaCO_3$ precipitation assay. In fact both extracts affected the final morphology of the crystals, moreover pearls protein was able to precipitate and stabilize vaterite, while irregular calcite was obtained using the shell extract. A possible explanation of this difference in polymorphs determination can be found in the higher number of glycosilation of pearls protein. Marie et al. (Marie B., 2007) have already demonstrated how after removal of the polysaccharides from shells proteins, their effect on precipitation was dramatically altered and the calcium binding activity lost.

The precipitation assay furnished another important evidence: the glycoproteins interact with the inorganic phase since the preliminary nucleation step. In fact the polypeptides were found both on the surface and inside the crystals. This allows postulating a direct and high specific control of the proteins starting from nucleation and continuing during the growth of calcium carbonate. In thermodynamic terms, is also possible to think that the polypeptides can lower the lattice energy in the crystals, exercising in this way a control on the polymorphism. A previous work (Levi Y., 1998) has already described that the macromolecular mediated polymorphs regulation can be exerted during nucleation step. The influence on nucleation, probably linked to the Ca^{++} binding activity, can explain the occurrence of the additional layers on control crystals when several precipitations were effected in presence of the extracts. The idea that these glycoproteins can be the main regulator in the crystallization is also corroborated by the observation of the inhibitory effect of the PoAb-glycoPe48 and the absence of effect when acetazolamide was added in the reaction. The last finding can exclude the involvement of carbonic anhydrase in polymorph selection even not underestimating the relevance of its catalytic activity in bio-calcification. We finally recognized the soluble proteins isolated from shells and pearls as main regulators of polymorph selection in the discussed *in vitro* crystallization experiments. Other works have also focused on the role

of aminoacids as aspartic acid or leucine; on the occurrence of inhibitors of a specific polymorphic structure and on other matrix components as β-chitin or silk fibroin-like proteins (Levi Y., 1998, Falini G., 1996). The present study together with previous remarkable findings, gives more clues for understanding the extremely complicate but challenging phenomenon of calcium carbonate biomineralization. For sure the deduced conclusions are referred to extremely simplified conditions; in the natural environment, more factors should be taken in consideration, as the interaction between all the components of the organic matrix or the parameters of the water like: temperature, pollution, salinity and the presence of inorganic ions especially magnesium and strontium (Watabe N., 1974).

The unique features of the biologically formed minerals (Weiner S., 1997) increase the interest in understanding the mechanisms exploited by biological systems in minerals synthesis. The reported enzymatic activity together with the possibility to stabilize high energetic polymorphs, offer new tools for producing innovative biomaterials for various applications. Industry is looking forward to using novel hybrid materials inspired in natural ones. Calcium carbonate for example, is extensively utilized in water treatment (scaling), in rubber, plastic, paper, paints production as filler and enhancer for gloss, brightness, whiteness, smoothness and mechanical property. It can improve the dispersibility, dissolvability and rheological property of target products, optimizing their performance and lowering the costs as well. In pharmaceutical industry calcium carbonate is used as bulking agents; as anti-acid in gastric and duodenal ulcer; as calcium supplement to prevent osteoporosis and to treat high phosphate levels in patients with kidney disease.

The opportunity to take advantage of the organic control in polymorph selection, self-assembly and regulation of crystallization can be the new successful strategy for the future. Polymorphs have different physical-chemical properties, for example during printing processes the application of different types of calcium carbonate, used as additive in paper or ink, can results in a different colour and lustre (Kitamura M., 2001). Vaterite has high specific surface area, high solubility, high dispersion and small specific gravity compared with the other two crystal phases (Naka N., 2002). Polymorphs selection can be an advantage in pharmaceutical formulations: changes in

polymorphic form can affect the solubility and morphology regulating the bioavailability of the drugs (Kralj D., 1990; Mann S., 1995; DickinsonS.R., 2002).
These effects render the different phases of calcium carbonate promising components for drug delivery systems.
Stable polymorphs are difficult to predict and obtain (Wei Chew J., 2007); the protein isolated from pearls not only offers the possibility to select and stabilize vaterite but also, being included in the crystals, gives to the biominerals enhanced features as high thermal stability and low dissolubility, making this *biovaterite* unique. (Quiao L., 2008).
Another promising application of nacre and its soluble extract is in restoration or replacement of damaged bones as biointegrated materials with high compatibility and osteoinductive effects (Silve C., 1992, Almeida M.J., 2001). For these reasons many research groups are focusing their study on the mechanisms that control biomineralization (Addadi L., 2006). Elucidation of the function of the organic components is the way to reproduce *in vitro* the same control in crystal growth from the angstrom to the millimetres levels. Together with the techniques of molecular biology and the production of recombinant proteins will be possible to produce environmental friendly materials, with hierarchical organization, self organized structures and controlled morphology.

6. SUMMARY

Pearls are an amazing example of calcium carbonate biomineralization. They show a classic *brick and mortar* internal structure in which the predominant inorganic part is composed by aragonite and vaterite tablets. The organic matrix is disposed in concentric layers tightly associated to the mineral structures. Freshwater cultivate pearls (FWCPs) and shells nacreous layers of the Chinese mussel *Hyriopsis cumingii* were demineralized using an ion exchange resin in order to isolate the organic matrix. From both starting materials a soluble fraction was obtained and further analyzed. The major component of the soluble extracts was represented by a similar glycoprotein having a molecular weight of about 48 kDa in pearls and 44 kDa in shells. Immunolocalization showed their wide distribution in the organic sheet surrounding calcium carbonate tablets of the nacre and in the interlamellar and intertabular matrix. These acidic glycoprotein also contained inside the aragonite platelets, are direct regulators during biomineralization processes, participating to calcium carbonate precipitation since the nucleation step. Selective calcium carbonate polymorph precipitation was performed using the two extracts. The polysaccharides moiety was demonstrate to be a crucial factor in polymorphs selection. In particular, the higher content in sugar groups found in pearls extract was responsible of stabilization of the high energetic vaterite during the *in vitro* precipitation assay; while irregular calcite was obtained using shells protein. Furthermore these polypeptides showed a carbonic anhydrase activity that, even if not directly involved in polymorphs determination, is an essential regulator in $CaCO_3$ formation by means of carbonate anions production. The structural and functional characterization of the proteins included in biocomposites, gives important hints for understanding the complicated process of biomineralization. A better knowledge of this natural mechanism can offer new strategies for producing environmental friendly materials with controlled structures and enhanced chemical-physical features.

7. ZUSAMMENFASSUNG

Biominerale sind Verbindungen aus anorganischen Mineralen mit Biomolekülen. Perlmutt ist ein klassisches Beispiel eines solchen Biominerals. Der mineralische Anteil besteht aus Aragonit- oder Vateritplättchen, die lateral in Schichten und vertikal in Stapeln angeordnet sind. Zwischen den einzelnen Plättchen, sowohl lateral wie auch vertikal, befindet sich die sogenannte organische Matrix.

Mittels Ionenaustauscher wurde Perlmutt aus Schalen und Perlen der Süßwassermuschel *Hyriopsis cumingii* demineralisiert und die organische Matrix gewonnen. Diese konnte aus beiden Ausgangsmaterialien als lösliche Proteinfraktion isoliert werden. SDS-Page-Analysen enthüllten in beiden Extrakten das Vorhandensein eines Hauptproteins, einem sauren Glycoprotein, dessen Molekulargewicht in Perlen bei 48kDa und in den Muschelschalen bei 44kDa liegt. Nach Entwicklung polyklonaler Antikörper gegen die Perlenglycoproteine konnte mit Hilfe von Immunfärbung ihre Verteilung in den Perlen und Muschelschalen ermittelt werden. Sie konnten sowohl in der organischen Schicht, welche die einzelnen Kalziumcarbonatplättchen umgibt, sowie in der interlamellaren und der intertabularen Matrix nachgewiesen werden. Diese sauren Glycoproteine, die auch innerhalb der Kalziumcarbonatplättchen nachweisbar sind, wirken als direkte Regulatoren im Verlauf des Biomineralisationsprozesses. Auch während der Kalziumcarbonatpräzipitation direkt nach der Kristallkeimbildung sind sie an der Ausbildung der Kristallmorphologie beteiligt. Es wurde nachgewiesen, dass die Morphologie der Kristalltypen von der Polysaccharidkomponente der Glycoproteine abhängig ist.

Es konnte gezeigt werden, dass der höhere Gehalt an Polysacchariden des 48kDa großen Proteins für die Stabilisation des hochenergetischen Vaterits während der Präzipitation *in vitro* verantwortlich ist, während das Protein aus der Schale zur Ausbildung des strukturloserem Calcit führt. Mit beiden Extrakten wurde jeweils eine selektive Kalziumcarbonatpräzipitation durchgeführt. Beide Polypeptide zeigten des Weiteren die Aktivität einer carbonischen Anhydrase, die zwar nicht direkt in den Prozeß der Formgebung involviert ist, aber ein essentieller Regulator der $CaCO_3$-Bildung darstellt, indem sie Carbonatanionen bildet. Die strukturelle und funktionelle Charakterisierung von Proteinen, die in Biokompositen enthalten sind, enthalten

wichtige Hinweise zur Aufklärung der komplizierten Prozesse der Biomineralisation. Ein besseres Verständnis dieses natürlichen Mechanismus kann neue Strategien für die Produktion umweltfreundlicher Materialien mit kontrollierter Strukturbildung und verbesserten chemisch-physikalischen Eigenschaften ermöglichen.

8. REFERENCES

Addadi L. and Weiner S. (1997) A pavement of pearl. *Nature,* 389, 6654, 912-915.

Addadi L., Weiner S. (1985) Interaction between acidic proteins and crystals: Stereochemical requirements in biomineralization. *Proc. Natl. Acad. Sci. USA* 82, 4110-4114.

Addadi L., Joester D., Nudelman F., and Weiner S. (2006) Mollusc shell formation: a source of new concepts for understanding biomineralization processes. *Chem. Eur. J.*, 12, 980-987.

Almeida M.J., Pereira L., Milet C., Haigle J., Barbosa M., Lopez E. (2001) Comparative effects of nacre water-soluble matrix and dexamethasone on the alkaline phosphatase activity of MRC-5 fibroblasts. *J. Biomed. Mater. Res.* 57, 2, 306-312.

Aizenberg J., Lambert G., Weiner S., Addadi L. (2002) Factors Involved in the Formation of Amorphous and Crystalline Calcium Carbonate: A Study of an Ascidian Skeleton. *J. Am. Chem. Soc.* 124, 32-39.

Akamatsu S., Zansheng L. T., Moses T. M., and Scarrat K. (2001) The current status of Chinese freshwater cultured pearls. *Gems & Gemology,* 37, 2, 96-113.

Anthony J.W., Bideaux R.A., Bladh K.W., and Nichols M. C. (2001-2005) Handbook of Mineralogy, version 1. Mineral Data Publishing, Tucson, Arizona.

Armstrong J.M., Myers D.V., Verpoorte J.A., Edsall J.T. (1966) Purification and properties of human erythrocyte carbonic anhydrase. *J. Biol. Chem.* 241, 5137-5149.

Barker R. (1973) The Reversibility of the reaction $CaCO_3 \leftrightarrow CaO + CO_2$. *J. Appl. Chem. Biotechnol.*, 23, 733.

Barker R. (1974) The reactivity of calcium oxide toward carbon dioxide and its use for energy storage. *J. Appl. Chem. Biotechnol*. 24, 221

Bäuerlein E. (2003) Biomineralization of unicellular organisms: an unusual membrane biochemistry for the production of inorganic nano- and microstructures. *Angew. Chem. Int. Ed. Engl.* 42, 614-640.

Becker A., Ziegler A. and Epple M. (2005a) The mineral phase in the cuticles of two species of Crustacea consists of magnesium calcite, amorphous calcium carbonate, and amorphous calcium phosphate. *Dalton Trans.* 1814 – 1820.

Becker A., Sötje I., Paulmann C., Beckmann F., Donath T., Boese R., Prymak O., Tiemann H., Epple M. (2005b) Calcium sulfate hemihydrate is the inorganic mineral in statoliths of *Scyphozoan medusae* (Cnidaria). *Dalton Trans.* 21, 1545-1550

Bédouet L., Schuller M.J., Marin F., Milet C., Lopez E. and Giraud M. (2001) Soluble proteins of the nacre of the giant oyster *Pinctada maxima* and of the *Haliotis tubercolata*: extraction and partial analysis of nacre proteins. *Comp. Bioch. and Phys. Part B* 128, 389-400.

Bischoff J. L. (1968) Catalysis, inhibition and the calcite aragonite problem. II. The vaterite aragonite transformation. *Amer. J. Sci.* 266, 80-90.

Blank S., Arnoldi M., Khoshnavaz S., Treccani L., Kuntz M., Mann K., Grathwohl G. and Fritz M. (2003) The nacre protein perlucin nucleates growth of calcium carbonate crystals. *Journal of Microscopy* 212, 280-291.

Bosselmann F., Romano P., Fabritius H., Raabe D. and Epple M. (2007) The composition of the exoskeleton of two crustacea: the American lobster *Homarus americanus* and the edible crab *Cancer pagurus. Thermochimica Acta***.** 463, 1-2, 65-68.

Campbell K.P., MacLennan D.H., and Jorgensen A.O. (1983) Staining of the Ca^{2+}-binding proteins, calsequestrin, calmodulin, troponin c, and s-100, with the cationic carbocyanine dye "Stains-all". *JBC* 258, 18, 11267-11273.

Currey J.D. (1980) Mechanical properties of mollusc shell. Vicent J.F.V. and Currey J.D. Eds., Cambridge Univ. Press, Cambridge, 75-97.

Dan H. and Ruobo G. (2002) Freshwater pearl culture and production in China. *Aquaculture Asia*. 7, 1, 1-58.

DeLong E. F., Frankel R.B. and Bazylinski D. A. (1993) Multiple Evolutionary Origins of Magnetotaxis in Bacteria. *Science*, 259, 5096, 803 – 806.

Dickinson S.R., Henderson G.E, McGrath K.M. (2002) Controlling the kinetic versus thermodynamic crystallization of calcium carbonate. *Journal of Crystal Growth,* 244, 369-378.

Downs R. T., Bartelmehs K. L., Gibbs G. V., Boisen M. B. (1993) Interactive software for calculating and displaying X-ray or neutron powder diffractometer patterns of crystalline materials. *American Mineralogist* 78, 1104-1107.

Falini G., Albeck S., Weiner S., Addadi L. (1996) Control of aragonite or calcite polymorphs by mollusc shell macromolecules. *Science*, 271, 5245, 67-69.

Falini G., Fermani S., Vanzo R., Miletic Q., and Zaffino G. (2005) Influence on the formation of aragonite or vaterite by otolith macromolecules. *Eur. J. Inorg. Chem*. 1, 162-167.

Fendler J.-H. (1997) Biomineralization inspired preparation of nanoparticles and nanoparticulate films. *Current Opinion in Solid State & Material Science*, 2, 365-369.

Frankel R.B., Blakemore R.P. and Wolfe R.S. (1997) Magnetite in freshwater magnetotactic bacteria. *Science* 203, 4387, 1355-1356.

Fu G., Valiyaveettil S., Wopenka B., Morse D.E. (2005) $CaCO_3$ biomineralization: acidic 8-kDa proteins isolated from aragonitic abalone shell nacre can specifically modify calcite crystal morphology. *Biomacromolecules,* 6, 1289-1298.

Golberg H.A and Warner K.J. (1997) The staining of acidic proteins on polyacrylamide gels: enhanced sensitivity and stability of "Stains-All" staining in combination with silver nitrate. *Anal.Biochem* 251, 227-233.

Gotliv B.A., Addadi L. and Weiner S. (2003) Mollusc shell acidic proteins. In search of individual functions. *ChemBioChem* 4, 522-529.

Harlow E., Lane D. (1988) Antibodies, a laboratory manual. Cold Spring Harbor Laboratory

Hou W.T., Feng Q.L. (2006) Morphologies and growth model of biomimetic fabricated calcite crystals using amino acids and insoluble matrix membrane of *Mytilus edulis*. *Crystal Growth & Design* 6, 5, 1086-1090.

Hsi K.-L., Chen L., Hawke D.H., Zieske L.R. and Y P.-M. (1991) A general approach for characterizing glycosilation sites of glycoproteins. *Anal. Biochem.* 198, 238-245.

Kamhi S. R. (1963) On the structure of vaterite, $CaCO_3$. *Acta Crystallographica* 16 770-772.

Kaplan David L. (1998) Mollusc shell structures: novel design strategies for synthetic materials. *Current Opinion in Solid State & Material Science*, 3, 232-236.

Kitamura M. (2001) Crystallization and transformation mechanisms of calcium carbonate polymorphs and effect of magnesium ion. *J. on Colloid and Interface Science* 236, 318-327.

Kono M., Hayashi N., and Samata T. (2000) Molecular mechanism of the nacreous layer formation in *Pinctada maxima*. *Bioch. and Biophys. Research Comm*. 269, 213-218.

Kralj D. and Brecevic L. (1990) Vaterite growth and dissolution in aqueous solution I. Kinetics of crystal growth. *Journal of Crystal Growth* 104, 793-800.

Kroeger N., Poulsen N. (2007d) Biochemistry and molecular genetics of silica biomineralization in diatoms. In Baeuerlein E (ed.) *Handbook of Biomineralization; Vol. 1: Biological Aspects and Structure Formation*. Weinheim; Wiley-VCH, 43-58.

Laemmli U.K. (1970) Cleavage of structural proteins during the assembly of the head of bacteriophage T4. *Nature* 227, 680-685.

Levi C., Barton J.L., Guillemet C., Le Bras E. and Lehuede P. (1989) A remarkably strong natural glassy rod: the anchoring spicule of the *Monorhaphis* sponge. *J. Mater. Sci. Lett***.** 8, 337–339.

Levi Y., Albeck S., Brack A., Weiner S. and Addadi L. (1998) Control over aragonite crystal nucleation and growth: an in vitro study of biomineralization. *Chem. Eur*. J. 4, 3, 389-396

Li J., Wang G., Bai Z. and Yue GH. (2007) Ten polymorphic microsatellite from freshwater pearl mussel, *Hyriopsis cumingii*. *Molecular Ecology Notes* 7, 1357-1359.

Lowenstam H.A. and Abbott D.P. (1975) Vaterite: a mineralization product of the hard tissues of a marine organism (Ascidiacea). *Science* 188, 4186, 363 – 365.

Lowenstam H.A., Weiner S. (1989) On biomineralization. Oxford University press.

Ma C., Zhang C., Nie Y., Xie L., Zhang R. (2005) Extraction and purification of matrix protein from the nacre of pearl oyster *Pinctada fucata*. *Tsinghua Science and Technology* 10, 4, 499-503.

Ma H.Y., Lee I.-S. (2006) Characterization of vaterite in low quality freshwater-cultured pearls. *Materials Science and Engineering* C 26, 721-723.

Mahadevan-Jansen A. and Richards-Kortum R. R. (1996) Raman spectroscopy for the detection of cancers and precancers. *Journal of Biomedical Optics* 1, 1, 31-70.

Mann S. (1995) Biomineralization and biomimetic materials chemistry. *J.Mater.Chem*. 5, 7, 935-946.

Marie B., Luquet G., Pais De Barros J-P., Guichard N., Morel S., Alcazar G., Bollache L. and Marin F. (2007) The shell matrix of the fresh water mussel *Unio pictorum* (Paleoheterodonta,Unionoida). *FEBS Journal* 274, 2933-2945.

Marin F., Corstjens P., de Gaulejac B., de Vrind-De Jong E. and Westbroek P. (2000) Mucins and molluscan calcification. *JBC* 275, 27, 20667-20675.

Marin F., Luquet G. (2004) Molluscan shell proteins. *C.R.Pale*. 3, 469-492.

Marin F., Luquet G., Marie B., and Medakovic D. (2008) Molluscan shell proteins: primary structure, origin and evolution. *Current topics in developmental biology* 80, 6, 209-276.

Marxen J.C. and Becker W. (1997) The organic shell matrix of the freshwater snail *Biomphalaria glabrata*. *Comp. Biochem. Physiol.* 118B, 23–33

Matsushiro A. and Miyashita T. (2004) Evolution of hard-tissue mineralization: comparison of the inner skeletal system and the outer shell system. *J. Bone Miner. Metab*. 22, 163-169.

Mayer, Fritz K., Jena Z. (1932) The distribution of calcium carbonate in the animal kingdom with special reference to the invertebrates. *Naturw*. 66, 199-222.

McConnel J.D.C. (1960) Vaterite from Ballycraigy, Larne, Northern Ireland. *Mineralogical Magazine* 32, 534-544.

McCreery R.L. (2001) Raman spectroscopy for chemical analysis. *Meas. Sci. Technol.* 12, 653-654.

Meyer K.D., Paul V.J. (1995) Variation in secondary metabolite and aragonite concentration in the tropical green seaweed *Neomeris annulata:* effects on herbivores by fishes. *Marine Biology* 122, 537-545.

Michenfelder M., Fu G., Lawrence C., Weaver J.C., Wustman B.A., Taranto L., Evans J.S., Morse D.E (2003) Characterization of two molluscan crystal-modulating biomineralization proteins and identification of putative mineral binding domains. *Biopolymers* 70, 522-533.

Miyamoto H., Miyashita T., Okushima M., Takashi M., Nakano S. and Matsushiro A. (1996) A carbonic anhydrase from the nacreous layer in oyster pearls. *PNAS USA Genetics* 93, 9657-9660.

Miyamoto H., Miyoshi F. and Kohno J. (2005) The carbonic anhydrase domain protein nacrein is expressed in the epithelial cells of the mantle and acts as a negative regulator in calcification in the mollusc *Pinctada fucata*. *Zoological Science* 22, 311-315.

Miyashita T., Takagi R., Okushima M., Miyamoto H., Nishikawa E. and Matsushiro A. (2000) Complementary DNA cloning and characterization of pearlin, a new class of matrix protein in the nacreous layer of oyster pearls. *Marine Biotechnology* 2, 409-418.

Müller W.E.G., Belikov S.I., Tremel W., Schlossmacher U., Natoli A., Brandt D., Boreiko A., Tahir M.N., Mueller I.M. and Schroeder H.C. (2007d) Formation of siliceous spicules in demosponges: example *Suberites domuncula*. In Baeuerlein E (ed.) *Handbook of Biomineralization; Vol. 1: Biological Aspects and Structure Formation.* Weinheim, Wiley-VCH; 59-82.

Müller W.E.G., Rothenberger M., Boreiko A., Tremel W., Reiber A., Schröder H.C. (2005) Formation of siliceous spicules in the marine demosponge *Suberites domuncula*. *Cell Tissue Res*. 321, 285–297.

Naka K., Tanaka Y., Chujo Y. (2002) Effect of anionic starburst dendrimers on the crystallization of CaCO3 in aqueous solution: Size control of spherical vaterite particles. *Langmuir* 18, 9, 3655-3658.

Nehrke G., Van Cappellen P. (2006) Framboidal vaterite aggregates and their transformation into calcite: A morphological study. *Journal of Crystal Growth* 287, 2, 528-530.

Norizuki M., Samata T. (2008) Distribution and function of the nacrein-related proteins inferred from structural analysis. *Mar. Biotechnol*. 10, 234-241.

Oliveira A.M. , Farina M. , Ludka I.P. and Kachar B. (1996) Vaterite, calcite, and aragonite in the otoliths of three species of piranha. *Naturwissenschaften* 83, 3, 133-135.

Palchik N.A. and Moroz T.N. (2005) Polymorph modifications of calcium carbonate in gallstones *Journal of Crystal Growth***.** 283, 3-4, 450-456.

Qiao L., Feng Q.L. and Li Z. (2007) Special vaterite found in freshwater lacklustre pearls. *Crystal Growth & Design* 7, 2, 275-279.

Qiao L., Feng Q.L., Liu Y. (2008) A novel bio-vaterite in freshwater pearls with high thermal stability and low dissolubility. *Material Letters* 62, 1793-1796.

Robinson D.H., and Sullivan C.W., (1987) How do diatoms make silicon biominerals. *TIBS* 12, 151–154.

Samata T., Hatashi N., Kono M., Hasegawa K., Horita C., Akera S. (1999) A new matrix protein family related to the nacreous layer formation of *Pinctada fucata*. *FEBS Letters* 462, 225-229.

Sarikaya M. (1999) Biomimetics: Materials fabrication through biology. *PNAS* 96, 25, 14183-14185.

Sharma Y., Rao C. M., Rao S. C., Gopala Krishna A., Somasundaram T. and Balasubramanian D. (1989) Binding Site Conformation Dictates the Colour of the Dye Stains-all. *The Journal of Biological Chemistry*. 264, 35, 20923-20972.

Shen X., Belcher A.M., Hansma P.K., Stucky G.D. and Morse D. (1997) Molecular cloning and characterization of lustrin A, a matrix protein from shell and pearl nacre of *Haliotis rufescens*. *J. Biol. Chem*. 272, 32472-32481.

Silve C., Lopez E., Vidal B., Smith D.C., Camprasse S. And Couly G. (1992) Nacre initiates biomineralization by human osteoblasts maintained *in vitro. Calcif. Tissue Int*. 51, 363-369.

Spiro T.G. (1988) Biological applications of Raman Spectroscopy, Vol. 3: Resonance Raman spectra of heme proteins and other metalloproteins. John Wiley and Sons Inc., New York, NY.

Strack E. (2001) Perlen. Ruehle-Diebener Verlag, Stuttgart

Sudo S., **Fujikawa T**., **Nagakura T**., **Ohkubo T**., **Sakaguchi K**., **Tanaka M**., **Nakashima K**., **Takahashi T**. **(1997)** Structures of mollusk shell framework proteins. *Nature* 387, 563-564

Swift D.M. and Wheeler A.P (1992) Evidence of an organic matrix from diatom biosilica. *J. Phycol*. 28, 202–209

.

Switzer R.C., Merril C.R., Shifrin S. (1979) A highly sensitive silver stain for detection of nanogram levels of protein. *Anal. Biochem.* 239, 2, 223-37.

Taylor M.G., Simkiss K., Greaves G.N., Okazaki M. and Mann S. (1993) An X-ray absorption spectroscopy study of the structure and transformation of amorphous calcium carbonate from plant cystoliths. *Proceedings: Biological Sciences*, 252, 1333, 22, 75-80.

Treccani L., Mann K., Heinemann F., and Fritz M. (2006) Perlwapin, an abalone nacre protein with three four-disulfide core (whey acidic protein) domains, inhibits the growth of calcium carbonate crystals. *Biophysical Journal*, 91, 2601-2608.

Wada K. (1998) Formation and quality of pearls. *Journ. Gemmol. Soc. Japan*, 20, 47-56

Wartewing S., Neubert R.H.H. (2005) Pharmaceutical application of Mid-IR and Raman spectroscopy. *Adv. Drug Del. Reviews* 57, 1144-1170

Watabe N. (1974) Crystal growth of calcium carbonate in biological system. *Journal of Crystal Growth* 24/25, 116-122.

Webb M.A. (1999) Cell-Mediated Crystallization of Calcium Oxalate in Plants. *Plant Cell*, 11, 751-761.

Weber K, Osborn M (1969) The reliability of molecular weight determinations by dodecyl-sulfate polyacrylamide gel electrophoresis. *J. Biol. Chem*. 244, 4406–4412.

Wehrmeister U., Jacob D.E., Soldati A.L., Häger T. and Hofmeister W. (2007) Vaterite in freshwater cultured pearls from China and Japan. *J. Gemm*. 31, 5/6, 269-276.

Wei Chew J., Black S. N., Shan Chow P., Tan R. B. H and Carpenter K. J. (2007) Stable polymorphs: difficult to make and difficult to predict. *Cryst. Eng. Comm*. 9, 128-130.

Weiner S. (2008) Biomineralization a structural perspective. *Journal of Structural Biology* 163, 3, 229-234.

Weiner S. and Addadi L. (1997) Design strategies in biological materials. *J.Mater. Chem.*, 7, 5, 689-702.

Weiner S., Dove P.M. (2003) An overview of biomineralization processes and the problem of the vital effect. *Reviews in Mineralogy and Geochemistry*. Mineral Soc America.

Weiner S., Levi-Kalisman Y., Raz S. and Addadi, L. (2003) Biologically formed amorphous calcium carbonate. *Conn. Tissue Res*. 44, 214-218.

Weiss I.M., Kaufmann S., Mann K., and Fritz M. (2000) Purification and characterization of perlucin and perlustrin, two new proteins from the shell of the mollusc *Haliotis laevigata*. *Bioch. And Biophys. Research Comm*. 267, 17-21.

Weiss M.I., Tuross N., Addadi L., Weiner S. (2002) Mollusc larval shell formation: amorphous calcium carbonate is a precursor phase for aragonite. *Journal of Experimental Zoology* 293, 5 , 478 – 491.

Wheeler A.P. and Sikes C.S. (1984) Regulation of carbonate calcification by organic matrix. *Amer. Zool.,* 24:933-944

Wilbur K.M. and Jodrey L.H. (1955) Studies on shell formation v. the inhibition of shell formation by carbonic anhydrase inhibitors. *Biol. Bull*. 108, 359-365.

Wilt F.H. (1999) Matrix and mineral in the sea urchin larval skeleton. *Journal of Structural Biology* 126, 216-226.

Young J.R., Henriksen K. (2003) Biomineralization within vesicles: the calcite of coccoliths. *Reviews in Mineralogy and Geochemistry*. 54, 1, 189-215.

Yu Z., Xie L., Lee S., Zhang R. (2006) A novel carbonic anhydrase from the mantle of the pearl oyster (*Pinctada fucata*). *Comparative Biochemistry and Physiology Part B*, 143, 190-194.

9 LIST OF ABBREVIATIONS

ACC	Amorphous Calcium Carbonate
AD	*Anno Domini*
APS	Ammonium persulfate
Asn	Asparagine
BC	Before Christ
BCIP	5-bromo-4-chloro-3-indolyl phosphate disodium salt
BSA	Bovine Serum Albumin
BSD	Back Scattered Detector
°C	Degree Celsius
CA	Carbonic Anhydrase
cm	Centimeter
dH_2O	Distilled water
DMF	Dimethylformamide
DOC	Deoxycholic acid
ED	Electron Diffraction
FITC	Fluorescein isothiocyanate
FWCP	Freshwater cultured pearl
g	Gram
Gal	Galactosamine
h	Hour
HRTEM	High Resolution Transmission Electron Microscopy
IEF	Iso Electric Focusing
kDa	Kilo-Dalton
Km	kilometers
M	Molar (mol/l)
mA	Milliampere
min	Minute
ml	Milliliter
mm	Millimeter
mM	Millimolar
mW	Milliwatt
MWCO	Molecular Weight CutOff
NAc	N-Acetyl
NBT	4-Nitroblautetrazoliumchlorid
ng	Nanogram
nm	Nanometer
O.N.	Over Night
PAGE	Poly-Acrylamide-Gel-Electrophoresis
PAS	Periodic Acid Schiff
PBS	Phosphate Buffered Saline
PBS-T	Phosphate Buffered Saline-0.1% Tween 20
pH	*Potentia Hydrogenii*
pI	Isoelectric Point
PoAb	Polyclonal Antibodies
Ppt	Precipitation

PVDF	Polyvinylidendifluorid
rpm	Rounds per minute
RT	Room temperature
SDS	Sodium Dodecyl Sulfate
sec	Second(s)
SED	Secondary Electron Detector
SEM	Scanning Electron Microscopy
Ser	Serine
STEM	Scanning Transmission Electron Microscopy
SWCP	Seawater cultured pearl
Tab.	Table
TEMED	N,N,N´,N´-Tetramethylendiamin
Thr	Threonine
Tris	Tris-(hydroxmethyl)-aminomethan
Tween 20	Poly(oxyethylen)20-sorbitan-monolaurat
US$	United States Dollar
V	Volt
v/v	Volume/volume (Vol.%)
vs	*Versus* (against)
w/v	Weight/volume
WB	Western Blot
WGA	Wheat Germ Agglutinin
µg	Microgram
µl	Microliter
µm	Micrometer